The activation of aggresomal pathway in Coxsackievirus B3 infection

Johanna Matilainen

Master's Thesis

University of Jyväskylä

Department of biological and

environmental science

Cell- and molecular biology

19.08.2016

Preface

This Master's Thesis was carried in Varpu Marjomäki's group, under supervision of Paula Turkki. I want to thank Varpu for the opportunity to conduct my work in her group. It has been a great pleasure to work and learn in such inspirational working environment with dedicated professionals. Specifically, I want to thank my supervisor, Paula, for the inspiring project, sophisticated guidance and support during my study. I really feel that I was in good hands during the whole project.

I would also like to thank all the other members of the group for great, helpful and cheerful working atmosphere: Mari Martikainen, Mira Myllynen, Visa Ruokolainen, Marjo Haapakoski, Anniina Runtuvuori, Salla Mattola and Dhanik Reshamwala.

Jyväskylän yliopisto
Matemaattis-luonnontieteellinen tiedekunta

Pro gradu-tutkielman tiivistelmä

Tekijä: Johanna Matilainen

Tutkielman nimi: Aggresomireitin aktivoituminen Coxsackievirus B3 –infektiossa

English title: The activation of aggresomal pathway in Coxsackievirus B3 infection

Päivämäärä: 05.06.2016 **Sivumäärä:** 44 + 6

Laitos: Bio- ja ympäristötieteiden laitos

Oppiaine: Solu- ja molekyylibiologia

Tutkielman ohjaaja(t): Paula Turkki ja Varpu Marjomäki

Tiivistelmä:

Aggresomin muodostuminen on yksi solun puolustusmekanismeista, joka pyrkii estämään proteiinien haitallisen aggregoitumisen solulimassa. Aikaisemmat kokeet ovat näyttäneet, että ihmisen enterovirus-infektio aiheuttaa muutoksia vimentiinissä, tyypin III välikokoisessa filamentissa (Turkki et al., julkaisematon data). Nämä muutokset ovat hyvin samankaltaisia aggresomin muodostumisen aikana tapahtuvien muutoksien kanssa. Tämän tutkimuksen tarkoituksena oli selvittää mahdollisen aggresomin muodostumisreitin aktivoituminen Coxsackievirus B3 (CVB3) -infektiossa, ja hypoteesimme oli, että häkkimäisten vimentiinirakenteiden muodostumisen lisäksi myös muita aggresomin muodostumisreitin aktivoitumiseen yhdistettyjä tapahtumia voidaan havaita CVB3-infektoiduissa soluissa. Lisäksi arvioimme, että aggresomin muodostumisreitin aktivoituminen voi hyödyttää virusinfektiota tai isäntäsolua. Tutkimme työssä näitä aggresomin muodostumiseen liittyviä solumuutoksia infektoiduissa soluissa käyttämällä immunofluoresenssivärjäystekniikoita ja konfokaalimikroskopiaa. Tuloksemme osoittivat, että CVB3-infektio aiheuttaa häkkimäisen vimentiinirakenteen muodostumisen, ja että tämä rakenteellinen muutos vaatii mikrotubuluksia. Infektio aiheuttaa lisäksi suuria rakenteellisia muutoksia solulimakalvostoon ja Golgin laitteeseen, sekä ubikitiinin ja lämpöshokki (Hsp) 70 proteiinin siirtymisen perinukleaariseen tilaan. Tuloksemme viittaavat siihen, että aggresomireitti voi aktivoitua CVB3-infektiossa. Tietojemme mukaan aggresomireitin aktivoitumista ei ole aikaisemmin osoitettu tapahtuvan enterovirusten aiheuttamien infektioiden aikana. Vaikka enteroviruksia on tutkittu kauan, niiden lisääntymiskierron kaikkia eri vaiheita ei tunneta täysin. Tutkimuksemme tulokset tarjoavat uutta tietoa enterovirus-isäntäsolu –vuorovaikutuksista.

Avainsanat: Coxsackievirus B3, aggresomi, ER-stressi, vimentiini

University of Jyväskylä
Faculty of Mathematics and Science

Abstract of Master's Thesis

Author: Johanna Matilainen

Title of thesis: The activation of aggresomal pathway in Coxsackievirus B3 infection

Finnish title: Aggresomireitin aktivoituminen Coxsackievirus B3 –infektiossa

Date: 05.06.2016 **Pages:** 44 + 6

Department: Department of Biological and Environmental Science

Chair: Cell and Molecular Biology

Supervisor(s): Paula Turkki and Varpu Marjomäki

Abstract:

Aggresome formation is a cellular defence mechanism that is triggered in order to prevent the accumulation of aggregated proteins in the cytoplasm. It has been previously shown that human enterovirus infection causes changes in vimentin, type III intermediate filament protein (Turkki et al., unpublished data), and these structural changes in vimentin resemble the ones induced during aggresome formation. The aim of this study was to investigate the possible activation of aggresomal pathway during Coxsackievirus B3 (CVB3) infection. The hypothesis was that in addition to a vimentin cage, also other factors of the aggresomal pathway might be involved in viral infection, either for the benefit of the virus or host cell. We investigated these cellular changes by using immunofluorescent techniques and confocal microscope imaging. Our results illustrated that CVB3 infection causes a cage-like vimentin, and this rearrangement is dependent on microtubules. In addition, CVB3 infection was shown to induce major structural changes in the ER and Golgi apparatus, accompanied by the translocation of ubiquitin and Heat shock protein (Hsp) 70 to the perinuclear region. These observations indicated that aggresomal pathway could be involved in CVB3 infection. To our best knowledge, the utilization of aggresomal machinery by enteroviruses has not been shown earlier. Despite the fact that enteroviruses have been under research for a long time, there are still areas of the viral lifecycle that are poorly known. Our findings provide more information about enterovirus-host cell –interactions.

Keywords: Coxsackievirus B3, aggresome, ER stress, vimentin

Table of contents

Abbreviations

A549 cells	Human lung carcinoma cells
AFSV	African swine fever virus
CAR	Coxsackievirus and adenovirus receptor
CMV	Cytomegalovirus
CVB3	Coxsackievirus B3
DAF	Decay-accelerating factor
DMEM	Dulbecco's Modified Eagle Medium
ER	Endoplasmic Reticulum
FBS	Fetal bovine serum
GFAP	Glial fibrillary acidic protein
Hsp70	Heat shock protein 70
HeLa cells	Human cervical cancer cells
IF	Intermediate filament
MTOC	Microtubule organizing center
PBS	Phosphate buffered saline
PFA	Paraformaldehyde
UPR	Unfolded protein response

1. Introduction

1.1. Enteroviruses

Enteroviruses are small, (about 30 nm in diameter) positive sense, single-stranded RNA viruses belonging to the *Picornaviridae* family. Nonenveloped, icosahedral protein capsid is formed by four proteins, named VP1 to VP4. The outer surface is composed of proteins VP1, VP2 and VP3, while VP4 is found from the inner surface of the capsid. Historically, enteroviruses have been classified by their pathogenicity: the polioviruses, group A and B coxsackieviruses and echoviruses (Cherry and Krogstad, 2010). Recently, based on the genomic data, categorization by the pathogenicity has been questionned, and new identified enteroviruses (68-71) have been included to the same genus by only numbering them in the order of identification (For a review, see Hyypia et al., 1997). Probably one of the most well-known and studied human enteroviruses, poliovirus, is the causative agent of poliomyelitis. In the 20th century, epidemics caused by poliovirus took thousands of lives and even higher number of victims were left paralyzed. Despite the efforts to eradicate poliomyelitis, the disease still remains endemic in Pakistan and Afghanistan (WHO, 2016). The intensive study of poliovirus and other picornaviruses has led to model system which has increased our understanding of the replication of RNA viruses.

Enteroviruses are one of the most common human pathogens. In addition to humans, they can infect other primates and a few domestic animals (Knowles et al., 2010). Most enterovirus infections are transmitted by fecal-oral or respiratory route. The primary replication takes place in the nasopharynx and alimentary canal tissues, from which virus can then spread to other locations (For a review, see Harris and Coyne, 2014). Syndromes caused by enteroviruses vary strongly both in severity and nature: For example, Human rhinovirus infection is restricted to respiratory mucosa, leading to mild, upper respiratory symptoms, whereas human Coxsackievirus B4 can cause inflammatory pancreatic disease (For a review, see Abzug, 2014; Lansdown, 1976). Asymptomatic diseases leading to more severe neurological illnesses and myocarditis are also included in the diverse medical conditions caused by enteroviruses. Generally enteroviruses cause acute, lytic infections, but persistent infections have been observed both *in vivo* and *in vitro* (Schnurr and Schmidt, 2013). Recently the connection between persistent enterovirus infections and the

development of type 1 diabetes has become a huge interest in research (For a review, see Haverkos et al., 2003).

1.1.1. **Coxsackievirus B3**

Coxsackievirus B3 (CVB3) is one of the six serotypes of coxsackievirus B viruses (CVB), named CVB1 to CVB6. CVB3 uses the coxsackievirus and adenovirus receptor (CAR), a transmembrane protein on the cell surface, to enter the host cell (Bergelson et al., 1997). Some CVB serotypes, including CVB3, also bind to decay accelerating factor (DAF), a GPI-anchored protein on the apical surface of polarized cells (Bergelson et al., 1995). In polarized cells, where CAR is located on the tight junction and is thus unavailable for the virus binding, CVB3 needs DAF for its transport to the tight junction (For a review, see Marjomaki et al., 2015). Thus in polarized cells, in addition to internalization, DAF is involved in other steps of the viral lifecycle, e.g. in initiating of kinase signals that are required for the infection in these cell types. However, CVB3 can not cause infection via DAF alone (Shafren et al., 1997; Coyne and Bergelson, 2006). Once the virus has been delivered to CAR, the formation of the intermediate particle is initiated (Coyne and Bergelson, 2006). In epithelial cells, CVB3 enters the host cell by caveolin-dependent, but dynamin-independent endocytosis. Whereas in polarized endothelial cells, the virus entry involves dynamin, the release of Ca^{2+} and calpain activity (For a review, see Marjomaki et al., 2015).

After the virus entry into the cytoplasm, the single-stranded 7.5 kb RNA genome is translated and transcribed. After initial translation, the viral polypeptide is synthesized and then cleaved into structural and nonstructural proteins by viral 2A and 3C proteases (For a review, see Garmaroudi et al., 2015). 3D RNA polymerase is required for the synthesis of negative-strand RNA that forms a template for positive-sense genome. Finally, structural proteins assemble around the RNA genome, resulting in a complete virion. Like many other enteroviruses, CVB3 also needs to modulate anti- and proapoptotic signals in order to complete the viral life cycle before the apoptosis that virus utilizes for the efficient egress and spread (For a review, see Harris and Coyne, 2014). In HeLa cells, caspase- and mitochondria-mediated apoptosis can be triggered by transient overexpression of viral 2A and 3C proteases (Chau et al., 2007).

In vivo, CVB3 infection affects several tissues, but the virus load is significantly higher in the heart compared to other organs (Cheung et al., 2005). Lytic CVB3 infection in the cardiac tissue can lead to acute myocarditis. In addition to lytic infection, similarly among other enteroviruses, CVB3 can also cause persistent infection. Interestingly, Pinkert et al. (2011) have shown that carrier-state, persistent CVB3 infecion in cardiomyocyte cells can occur, and this has been linked to the absence of CAR.

1.2. Intermediate filaments

Cytoskeletal proteins of all eucaryotic cells include polar microfilaments and microtubules. However, the third type of cytoskeletal proteins, intermediate filaments (IFs), are only found from cells of multicellular animal species, typically from the cytoplasm of cells that encounter mechanical stress. IFs are approximately 10-12 nm in diameter, meaning that they are intermediate in size between microfilaments and microtubules. Individual IF monomers contain a highly conserved α-helical rod domain that consists of four segments (1A, 1B, 2A and 2B, Figure 1) (For a review, see Herrmann and Aebi, 2000). These heptad repeat-containing segments are joined by L1, L12 and L2 –linkers. The rod domain is flanked by ”head” and ”tail” domains, and two of these monomers form a coiled-coil, nonpolar dimer, which serves as a basic subunit of IF structure. The differences in the sequences of ”head” and ”tail” domains vary between different IF types.

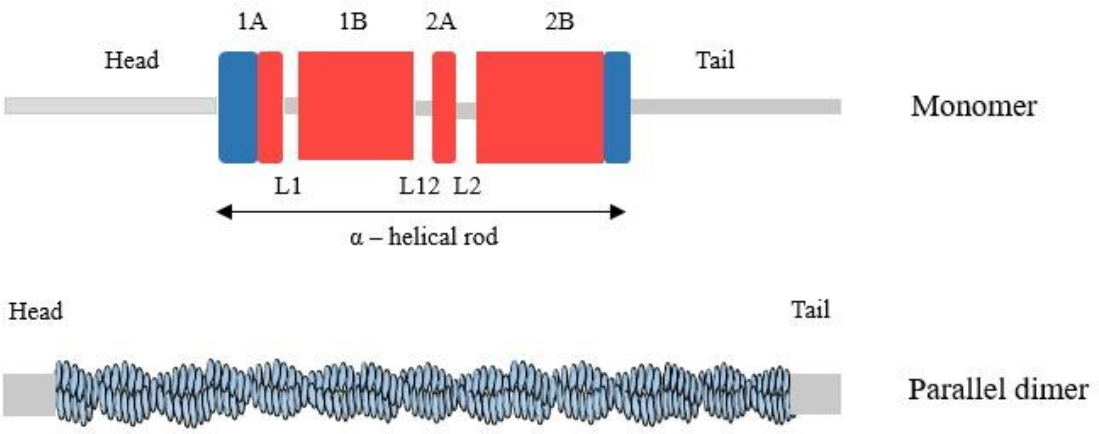

Figure 1. Structure of intermediate filaments. Intermediate filament monomer contains a highly conserved α-helical rod domain, that consists of four segments: 1A, 1B, 2A and 2B. These segments are joined by L1, L12 and L2 –linkers. Modified from Tang, (2008) and Kim and Coulombe, (2007). Made by utilizing Servier MedicalArt Powerpoint image bank (http://www.servier.com/Powerpoint-image-bank).

IFs are encoded by 65 genes, and the family of proteins constituting IFs includes over 40 different proteins that can be classified into five classes (For a review, see Herrmann and Aebi, 2000; Hesse et al., 2001; Table 1). Keratins are the most diverse IFs, as they comprise the first two goups of the IF family. Keratins are the most abundant structural proteins in all human epithelial cells forming single-layer epithelia and complex multi-layer epithelium. The third class includes desmin, vimentin, glial fibrillary acidic protein (GFAP) and peripherin. Desmin is expressed in all muscle cells, GFAP in astrocytes, and peripherin in some neurons. Axonal neurofilament proteins, e.g. NF-L, NF-M, and nestin comprise the fourth class of IFs. Nuclear lamins A, B and C form the fifth class of the IF family.

Table 1. Intermediate filaments. Modified from Herrmann and Aebi, (2000).

Type	Protein	Size (in kDa)	Distribution
I	Acidic cytokeratins	40 – 64	All epithelia
II	Basic cytokeratins	52 – 68	All epithelia
III	Vimentin	55	Cells of mesenchymal origin
	Desmin	53	Muscle cells
	Glial fibrillary acidic protein (GFAP)	50 – 52	Glia cells, astrocytes, stellate cells of liver
	Peripherin	54	Neuronal cells
IV	Alpha-Internexin	56	Neurons
	Nestin	240	Neutoepithelial stem cells, muscle cells
	NF-L	68	
	NF-M	110	Neurons
	NF-H	130	Neurons
	Neurofilament triplet proteins		Neurons
V	Lamins A	62 – 72	Most differentiated cells
	Lamins B	65 – 68	All cell types
	Lamins C	62 – 72	Most differentiated cells

In addition to structural support, IFs participate in the regulation of cell growth, survival, polarity, proliferation and gene regulation. They are also related to the regulation of apoptosis via interactions with several cellular proteins. Moreover, several IFs have roles in positioning cell organelles (e.g. mitochondria and the Golgi apparatus) and in maintaining their shape and function (For a review, see Toivola et al., 2005). They interact with microtubules, F-actin and other major components of cellular architecture. Despite the nonpolarity of IFs, at least vimentin cargo interacts with molecular motors (Helfand et al., 2002). IF function and dynamics are regulated by several modifications, including phopshorylation, farnesylation, glycosylation, transglutamination, as well as by an interaction with numerous binding proteins (For a review, see Omary et al., 2004). Recently, our understanding of the importance of IFs in genetic diseases has evolved: Over 30 human disorders, e.g. skin disorders and desmin myopathy, are related to mutations in genes encoding IFs.

1.2.1. **Vimentin**

Vimentin is a 57 kDa protein of the type III IF protein family expressed in a wide range of cells of mesenchymal origin. Similarly to other IFs, the α-helical rod domain is flanked by ”head” and ”tail” domains, and is comprised of four segments: 1A, 1B, 2A and 2B (Goldie et al., 2007). Vimentin forms a flexible and dynamic network in the cytoplasm, and in addition to maintaining tissue integrity, it is involved in many cellular functions, such as cell migration, attachment, signaling, apoptosis, immune defence and the regulation of genomic DNA (For a review, see Ivaska et al., 2007). Furthermore, vimentin has also been associated with lipid metabolism and the regulation of angiogenesis (For a review, see Schweitzer and Evans, 1998 and Dave and Bayless, 2014). Increased vimentin expression is one of the best indicators of epithelial-to-mesenchymal-transition (EMT), which is associated with many tumorigenic events. Increased vimentin expression has been related to many tumor tissues of several cancers, including breast and prostate cancer.

Several phosphatases and kinases phosphorylating vimentin have been identified, implying that this posttranslational modification is one of the most important regulators of vimentin dynamics and function known so far (For a review, see Dave and Bayless, 2014). Phosphorylation sites, usually serines, have been specifically associated with different cellular events, including stress, mitosis and differentiation. In addition, some other posttranslational modifications, such as citrullination and symoylation, have also been found to regulate vimentin. Vimentin can also serve as a substrate for several caspases, leading to vimentin fragments, irreversible disruption of vimentin network, and eventually to apoptosis (Byun et al., 2001).

Vimentin has recently been shown to be involved in many viral infections, at different steps of the viral lifecycle. It has been suggested that vimentin may be utilized as a receptor during virus infection, like with Human Immunodeficiency virus type 1 (HIV-1), Porcine Reproductive and Respiratory Syndrome Virus (PRRSV) and Enterovirus 71 (Thomas et al., 1996; Kim et al., 2006; Du et al., 2014). Vimentin has also been reported to be involved in the replication, transportation or production of e.g. Junin virus and Human Cytomegalovirus (CMV) infections (Kim et al., 2006; Miller and Hertel, 2009; Cordo and Candurra, 2003). The collapse of vimentin network into the perinuclear region has been observed during HIV-1, Theiler’s virus and African swine fever virus (ASFV) infections (Karczewski and Strebel, 1996; Nedellec et al., 1998; Stefanovic et al., 2005). The

involvement of vimentin in viral infection has been under research for a few decades, but little is still known about it's actual roles and importance in infection.

1.3. Aggresome formation

Misfolded proteins resulting from errors during protein translation and folding, as well as cellular stress can interfere with normal cellular functions, and are thus potentially toxic. To prevent their accumulation and aggregation in the cytoplasm, cells use molecular chaperones to aid in the folding of the proteins and proteosomal degradation to destroy harmful proteins (For a review, see Kopito, 2000). However, when the degrading capacity of proteasome is exceeded, misfolded proteins form insoluble aggregates in the cytoplasm. These are then transported along microtubules to the microtubule organizing center (MTOC), where they are packed into a large structure termed aggresome. Aggresomes usually appear as a spherical structure with a diameter of 1-3 µm, enriched in components of proteasomes and surrounded by a cage-like vimentin structure (For a review, see Garcia-Mata et al., 2002). Protein aggregate movement to the MTOC involves intact microtubule cytoskeleton and minus-end-directed dynein motors, as shown with nocodazole treatment and p50/dynamitin overexpression that keep aggregates distributed in the cytoplasm (Garcia-Mata et al., 1999; Johnston et al., 1998). Transportation machinery also involves a microtubule-associated deacetylase, HDAC6, which binds both to misfolded proteins and dynein motors, and thereby recruits protein aggregates for transportation to the MTOC (Kawaguchi et al., 2003).

During the aggresome formation, several cellular components and proteins are recruited to the MTOC (Figure 2). For example, various chaperones, enzymes involved in ubiquitination and components of proteasomes have been found. Chaperones involved in aggresome formation include several members of major chaperone families: Heat shock protein (Hsp) 70, Hsp90, and Hdj1 and Hdj2 from the Hsp40 family (Garcia-Mata et al., 1999; Wigley et al., 1999). Chaperonin TriC/TCP, alpha-synuclein, 14-3-3 and in some cases, ER luminal chaperone BiP/GFP78 also seem to colocalize with aggresomes (Waelter et al., 2001; Junn et al., 2002). In addition to chaperones, proteasomal particles are also related to components that are recruited during aggresome formation. Proteasomal components often get ubiquitinated, and ubiquitin is, indeed, also found from cystic

fibrosis transmembrane conductance regulator (CFTR) and presenilin-1 (PS1) -induced aggresomes (Johnston et al., 1998). Although ubiquitin is often related to aggresome formation, it has been reported that ubiquitin recruitment is not induced in the aggresome formation caused by GFP-250, mutant superoxide dismutase (SOD) or ATP7N (Garcia-Mata et al., 1999; Harada et al., 2001). Aggresome formation has also been reported to induce the recruitment of mitochondria to the perinuclear region and the disorganization of the Golgi apparatus which has been reported to surround the aggresome (For a review, see Garcia-Mata et al., 2002; Garcia-Mata et al., 1999).

As some viruses have been shown to utilize aggresomal machinery and to induce changes similar to the ones occuring during aggresome formation, the role of aggresomal pathway in viral infection has been under research for the last decade. ASFV assembles in viral factories that trigger highly similar events to the changes induced during aggresome formation, e.g. a cage-like vimentin, suggesting that ASFV utilizes the aggresomal pathway activation to concentrate viral particles to the assembly site (Heath et al., 2001). In addition, it has recently been reported that aggresomal machinery is essential for Influenza A virus uncoating and cell entry (Banerjee et al., 2014).

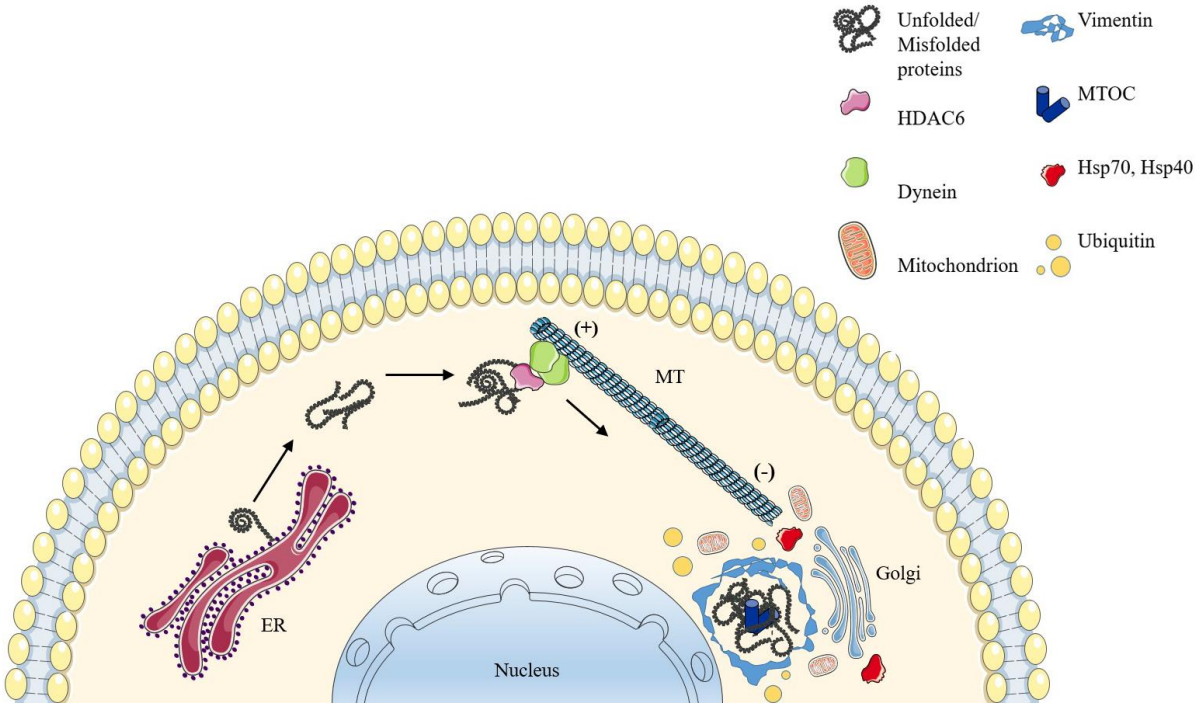

Figure 2. Aggresome formation. Unfolded or misfolded proteins that are translocated from the endoplasmic reticulum (ER), originated from polysomes or the cell stress, form aggregates in the cytoplasm. These protein aggregates are transported along microtubules (MT) to the perinuclear region where the aggresome formation occurs. Microtubule-dependent transport involves minus-end-directed dynein motor complex and a microtubule-associated deacetylase (HDAC6). The aggresome forms around the microtubule organizing center (MTOC) and is surrounded by a vimentin cage. Several cellular components are recruited to the perinuclear region during aggresome formation, e.g. Heat shock protein (Hsp) 70 and 40, and mitochondria. In addition, aggresomes can also get ubiquitinated. The Golgi apparatus has been reported to get displaced and localized around the aggresome. Modified from Garcia-Mata et al., (2002). Made by utilizing Servier MedicalArt Powerpoint image bank (http://www.servier.com/Powerpoint-image-bank).

1.4. ER stress

Abnormal accumulation of unfolded or misfolded proteins in the endoplasmic reticulum (ER) can lead to/cause ER stress. As a cytoprotective event, unfolded protein response (UPR) is triggered, leading to increased expression of binding immunoglobulin protein, BiP/GRP78. This molecular chaperone is the key regulator of signalling molecules involved in the ER stress pathway: inositol-requiring enzyme 1 α (IRE1α), protein kinase RNA-like ER kinase (PERK) and activating transcription factor 6 (ATF6) (For a review, see Sano and Reed, 2013). In order to alleviate extreme and prolonged ER stress that can potentially lead to apoptosis, these regulators are activated. As a result, refolding of misfolded proteins by chaperones is enhanced, the entry of newly synthesized proteins into

the ER is inhibited, proteins are translocated to the cytosol for ubiquitin-mediated degradation, and the autophagic pathway is activated. The most common modulators of the ER stress pathway can be found in the figure (Figure 3).

Recently, it has been demonstrated that many viruses can cause ER stress in infected cells (For a review, see He, 2006 and Zhang and Wang, 2012). ER stress can be induced by exploitation of the ER membranes, sabotage of the membranes during virion release, accumulation of viral proteins, and viroporins that lead to imbalance of calcium homeostasis of the host cell. Several RNA viruses, e.g. hepatitis C and poliovirus, replicate in the ER and cause rearrangements of membranes (El-Hage and Luo, 2003; Rust et al., 2001). Virus infection leads to efficient viral protein production in the host cell, and this high protein load can activate ER stress. Several viruses have been shown to activate one or more regulators of the ER stress pathway, and ER-mediated apoptosis (For a review, see He, 2006). ER stress can be induced as a protective response against viral infection and the inhibition of the ER stress pathway could enable virus infection. It is also possible that viruses utilize the ER stress pathway to induce apoptosis. Among human enteroviruses, enterovirus 71 and CVB3 have been shown to modulate the ER stress pathway (Jheng et al., 2012; Zhang et al., 2010). According to the study by Zhang et al., (2010), CVB3 induces the activation of BiP/GRP78, XBP1, ATF6 and CHOP-mediated apoptosis in cardiomyocyte and HeLa cells.

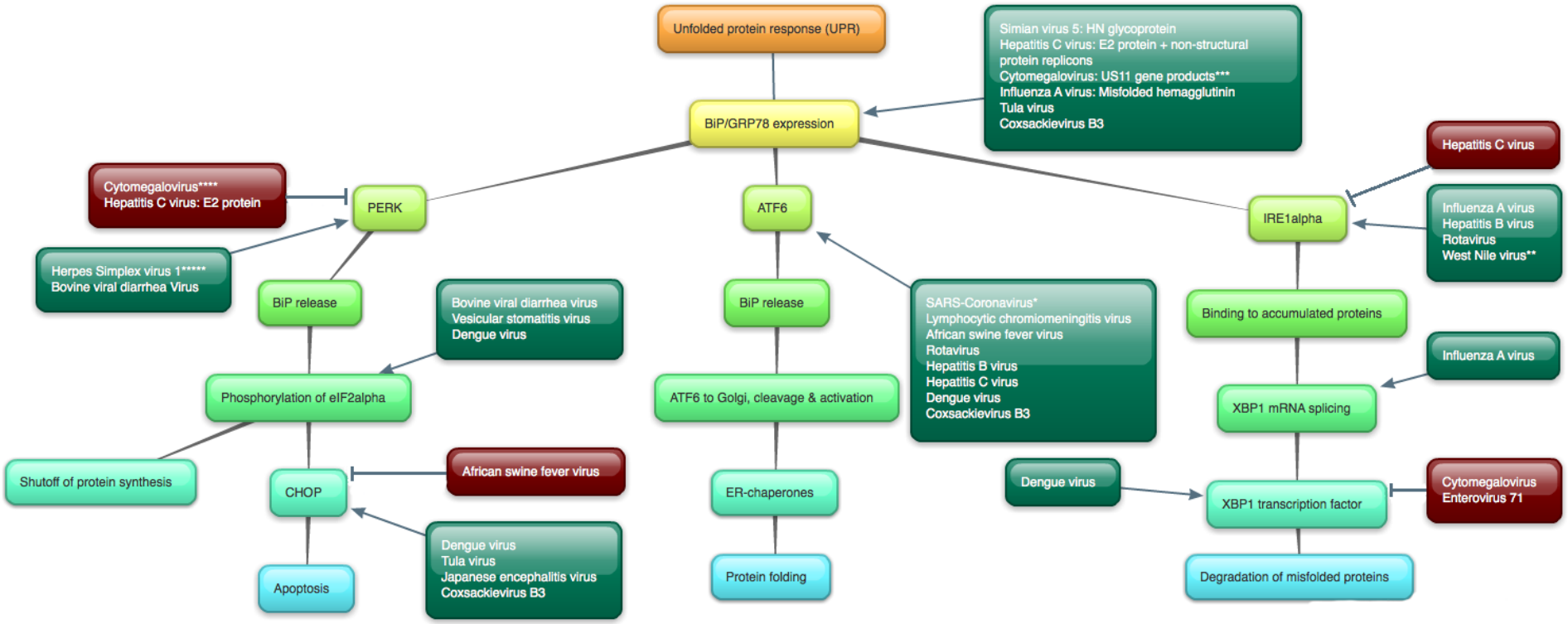

Figure 3. The endoplasmic reticulum (ER) stress signalling pathways. ER stress is induced by unfolded protein response (UPR), which activates the increased expression of ER-luminal BiP/GRP78 protein. The three main branches of the pathway, modulated by PERK, ATF6 and IRE1α, lead to decreased protein synthesis, increased protein degradation and expression of ER chaperones that mediate the refolding of proteins. Several viruses have been shown to modulate the ER stress pathway at different stages. Viruses in the red boxes inhibit or decrease the expression of factors of the pathway, and viruses in the green boxes induce the increased expresion or activity. SARS-Coronavirus*: 8ab accessory protein of SARS-Coronavirus has been reported to bind to the luminal domain of ATF6 and thus directly activate ATF6-mediated pathway. West Nile virus**: Although virus infection activates IRE1α-XPB1 pathway, the activation is not essential for the replication. Cytomegalovirus: US11 gene products***: Transient increase in BiP expression levels can be seen at the early stage of Cytomegalovirus replication. Cytomegalovirus****: PERK is only activated at the later stage of virus infection, not in the early phase. Herpes Simplex virus 1*****: Although PERK gets activated during virus infection, eIF2α remains unphopshorylated. Based on He, (2006); Jheng et al., (2012); Zhang and Kaufman, (2004).

2. Aim of the Study

In previous studies, Turkki et al. (unpublished data) have shown that enterovirus infection causes changes in vimentin, resulting in a ball or cage-like structure in the perinuclear region. This enterovirus-induced vimentin structure resembles the one occurring during aggresome formation. In fact, it has been reported that viruses can exploit aggresomal pathway for their replication and infection. Aggresome formation could also be triggered as a defence mechanism against viral infection. Due to the obvious resemblance between vimentin structures in aggresome formation and during enterovirus infection, we wanted to further study the possible role of the aggresomal pathway in the regulation of enterovirus infection. The main aims of this thesis were:

1. To form aggresomes artificially by using GFP-250 transfection in A549 cells

2. To investigate changes in cellular structures and key proteins associated with aggresome formation during lytic CVB3 infection in A549 cells

The hypothesis was that the activation of aggresomal pathway is triggered during CVB3 infection which is indicated by the similarity between cellular changes occurring in CVB3 infected cells and the ones induced in GFP-250 transfected cells.

3. Materials and methods

3.1. Cells

Human lung carcinoma (A549) and human cervical cancer HeLa MZ (HeLa) -cells were cultured in 80 cm^2 flasks at +37 °C, 5% CO_2. The growth medium contained Dulbecco's Modified Eagle Medium (DMEM, Thermo Fisher) with 10% Fetal Bovine Serum (FBS, Gibco, Life Technologies, United Kingdom), 1% GlutaMax and 1% penicillin and streptomycin. For the experiments, the cultures were washed with phosphate buffered saline (PBS) and incubated for 5 min at +37 °C with 2 ml of trypsin (Gibco, Life Technologies, United Kingdom) to detach the cells. The cells were then transferred into 12-well plates (the surface of each well was 3.8 cm^2) with coverslips on the bottom of each well and incubated at +37 °C, 5% CO_2 for o/n.

3.2. CVB3 infection

Cells in 12-well plates were infected with CVB3 (Nancy strain). First, cells were washed with PBS to remove serum residues and then infected with CVB3 (1/1500 dilution in 10% DMEM) for 5 h at +37 °C, 5% CO_2. The controls included uninfected cells that were treated with 10% DMEM only, but otherwise treated like the other samples. After incubation, cells were washed with PBS and fixed with 4% paraformaldehyde (PFA) for 30 min at RT. PFA was replaced with PBS and the coverslips were stored at +4 °C until immunolabeling.

3.3. GFP-250 transfection of CVB3-infected A549 and HeLa -cells

A549 and HeLa -cells in 12-well plates were transfected with GFP-250 plasmid by using Lipofectamine 2000 –transfection reagent (Invitrogen, Life Technologies, USA) according to manufacturer's instructions. Briefly, GFP-250 plasmid was diluted to DMEM, without any FBS, GlutaMax or penicillin/streptomycin (the final concentration 300 ng/µl per well). Transfection reagent was kept at RT for 30 min before the experiment. Transfection

reagent was diluted to DMEM, without any FBS, GlutaMax or penicillin/streptomycin. Diluted GFP-250 plasmid was added to transfection reagent dilution (the final concentration 6.9 ng/µl), and the plasmid-transfection reagent solution was incubated for 5 min at RT. 50 µl of the plasmid-transfection reagent solution was added to sample wells, and cells were incubated at +37 °C, 5% CO_2 for 24, 48 or 72 h. Cells were infected with CVB3 for 5 h before the end of transfections, as previously described. The control wells included the cells without any transfection treatment, the cells treated with transfection reagent dilution (without GFP-250 plasmid), GFP-250 transfected cells without CVB3 infection and CVB3-infected cells without GFP-250 transfection. Otherwise, the controls were treated similarly to the samples.

3.4. Immunolabelings

The cells were immunolabeled against γ-tubulin, ubiquitin, calreticulin, the trans-Golgi network (TGN) 46, vimentin, Hsp70, CVB3 capsid and viral replication intermediate double-stranded RNA (dsRNA). Antibody dilutions were made with 1.5% bovine serum albumin (BSA)/PBS 0.1% Triton X-100 as presented in the table (Table 2). Cells were permeabilized with 0.2% Triton X-100 in PBS for 5 min. Primary antibodies were labeled with appropriate fluorescence-conjugated secondary antibodies produced in goat (AlexaFluor® 488 or AlexaFluor® 555). The mounting of the immunolabeled coverslips was performed with Prolong® gold antifade reagent with DAPI (Molecular Probes, Life Technologies, USA).

Table 2. Antibodies and their final concentrations used in the experiments.

Primary/Secondary	Antibody	Final concentration	Origin
Primary	Rabbit anti-γ-tubulin	5 x 10^{-3} µg/ml	Bioss Antibodies, USA
Primary	Mouse anti-ubiquitin	1:200	Cell Signaling Technologies, USA
Primary	Rabbit anti-calreticulin	1:200	Thermo Fisher Scientific, USA
Primary	Rabbit anti-TGN46	1:150	Kind gift from George Banting, University of Bristol, UK
Primary	Mouse anti-vimentin	1:150	Leica Biosystems, Germany
Primary	Rabbit anti-vimentin	1:100	Abcam, UK
Primary	Rabbit anti-Hsp70	1:200	US Biological, USA
Primary	Mouse anti-dsRNA J2	1:8000	Thermo Fisher Scientific, USA
Primary	Rabbit anti-CVB3	1:200	Kind gift from Maija Meriläinen
Secondary	Goat anti-mouse AlexaFluor® 488 and 555	10 µg/ml	Molecular Probes Invitrogen, USA
Secondary	Goat anti-rabbit AlexaFluor® 488 and 555	10 µg/ml	Molecular Probes Invitrogen, USA

3.5. Nocodazole treatment of CVB3-infected A549 cells

A549 cells in 12-well plates were infected with CVB3 and treated with nocodazole. Nocodazole (final concentration 33 µM) dilution was made with 10% DMEM. Cells were infected with CVB3, and nocodazole was added either together with the virus or 1, 3 and 5 h after virus addition to the cells. First, cells were washed with PBS and then infected with CVB3 (Nancy strain, 1/1500 dilution in growth medium) for 1 h at +37 °C, 5% CO_2. The infection was let to proceed for 1 h, and after incubation the medium containing CVB3 was removed from the wells. Then, nocodazole was added so that all the samples were fixed at

the same time. Control cells included uninfected cells, CVB3-infected cells without any drug treatment, and uninfected cells that were treated with nocodazole for 6 h.

3.6. Confocal imaging

The coverslips were imaged with two microscopes with a resolution of 512 by 512 pixels per image: Olympus microscope IX81 with FluoView-1000 confocal setup (405-nm diode laser, 488-nm and 543-nm HeNe lasers) with a UPLSAPO 60x (numerical aperture [NA] 1.35) objective, and Nikon A1R Ti-E inverted microscope (405-nm diode laser, 488-nm argon laser, and 561-nm sapphire laser) with a CFI Apo VC 60XH ([NA] 1.4) objective.

3.7. Data-analysis with BioImageXD and statistical testing

The quantitative analyses of the confocal images were performed with BioImageXD software (Kankaanpaa et al., 2012). The threshold values for each channel (488 nm, 555 nm and 345 nm) were manually optimized to separate the signal from background in BioImageXD. To obtain total intensities of γ-tubulin, trans-Golgi network and viral particle signals, as well as the number of signal particles per cell, the relative amount of signal and particles were manually determined by dividing the total signal by the number of cells in an image. The total intensity of Hsp70 and the number of ubiquitin particles were quantified by using images that contained only one cell. The colocalization of Hsp70 signal with DAPI, showing the colocalization with the nucleus, was quantified by determining the percentage of colocalizing voxels.

Statistical testings were performed with GraphPad Prism -software. Comparisons were done with the unpaired Student t test with Welch's correction. As quantification results for the intensity of Hsp70 signal and the number of ubiquitin particles were obtained from several experiments, the data was normalized from different data sets to a common scale. All data is presented as means, and error bars represent the standard errors of the mean (SEM).

4. Results

4.1. GFP-250 induced aggresomes interfere with CVB3 infection

The main focus of this thesis was to investigate whether CVB3 infection could activate aggresomal pathway, or some steps of it, in A549 cells. The original plan was to form aggresomes artificially in cells by using the GFP-250 transfection (Garcia-Mata et al., 1999), and observe subsequent cellular changes during aggresome formation and in CVB3-infected cells with the aid of immunofluorescent techniques and confocal microscope imaging. However, despite the efforts to optimize the transfection, GFP-250 transfection induced aggresomes that were quite often found too large and also otherwise abnormal in A549 cells (data not shown). In addition, the transfection percentage was low. Strong GFP signal was often found inside the nucleus and all over the cytoplasm, rather than only in the perinuclear region, where aggresomes should form. According to confocal images, GFP-250 transfected cells were shrunken, usually contained highly fragmented nuclei, and were detached from the coverslip. Due to these, it was speculated that way too large aggresomes might have been cytotoxic to cells. In addition to A549 cells, we also studied GFP-250 transfection in HeLa cells for 24, 48 and 72 h, since HeLa cells normally have higher transfection percentage (Figure 4). GFP-250 expression was not significantly different in HeLa cells, as GFP signal was also found in the nucleus and cytoplasm of these cells. As with A549 cells, cells were small and the nuclei often looked fragmented, indicating that high expression levels might have been cytotoxic (Figure 4, indicated by arrows).

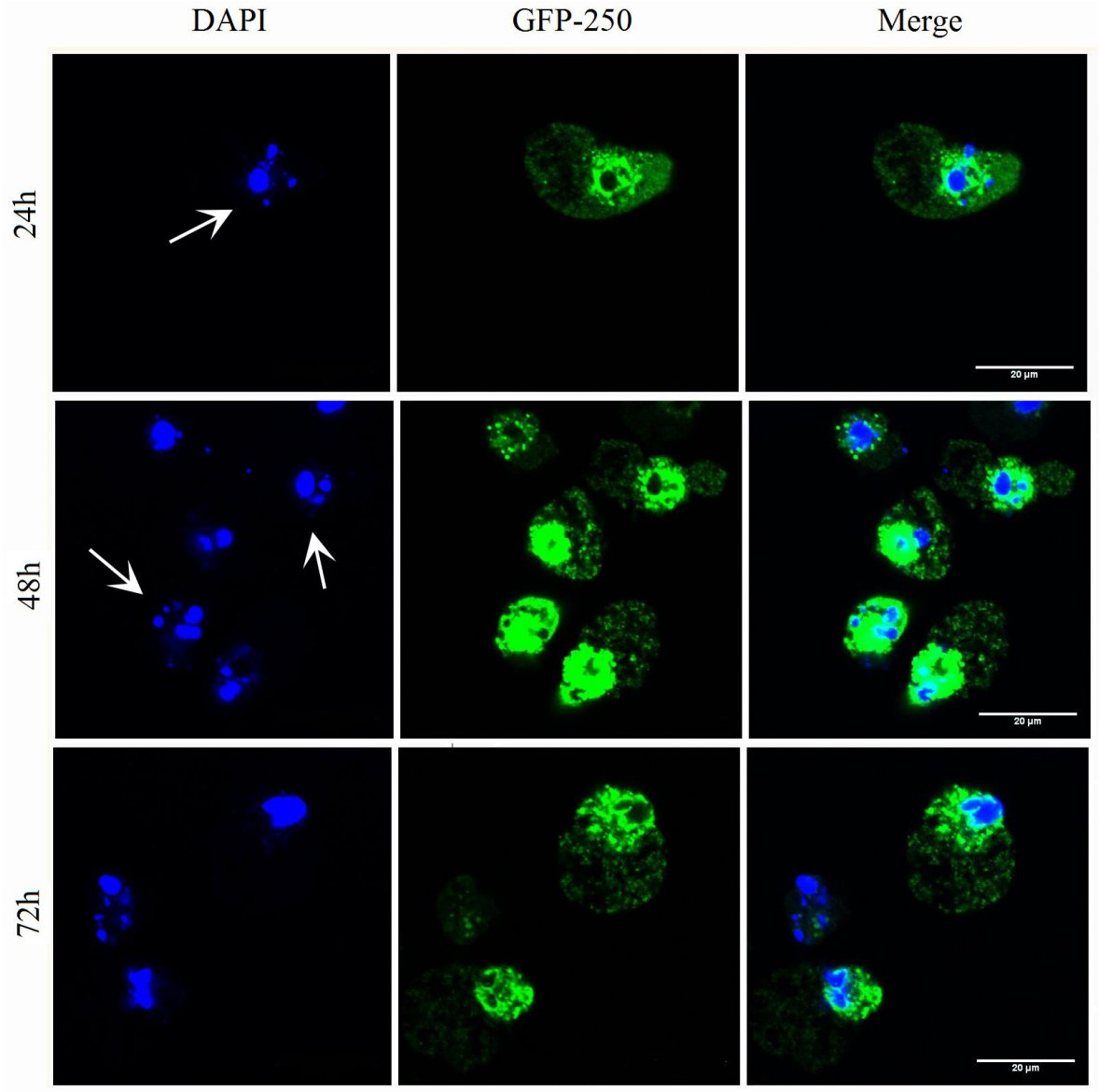

Figure 4. The optimization of GFP-250 transfection in HeLa cells. HeLa cells were transfected with GFP-250 –plasmid for 24, 48 and 72 hours and fixed. GFP-250 (green) resembles aggresomes that are formed during transfection. The nuclei of transfected cells were often fragmented (indicated by arrows). Cells were imaged with fluorescence confocal microscope. Cells are representative of one experiment, including approximately 105 analysed cells. Scale bars 20 µm.

Despite the fact that only few of the aggresome-containing cells looked healthy, we wanted to see what effect these aggresomes could have on infection. After 48 h transfection, A549 cells were infected with CVB3 for 5 h, fixed and immunolabeled for CVB3 capsid and viral replication intermediate dsRNA and imaged with fluorescence confocal microscope.

Transfected cells were identified by GFP-fluorescence, infected cells by the fluorescent labeling of virus capsid and viral dsRNA.

Nontransfected but infected cells showed large amounts of CVB3 capsid all over the cytoplasm (Figure 5, Ctrl, CVB3). Interestingly, CVB3 infection of transfected cells seemed unusual: CVB3 capsid –antibody colocalized with GFP-250, and the overall amount of virus capsid was extremely low (Figure 5, Transfection), suggesting that aggresomes might have captured viruses that have entered the cell and prevented the viral production.

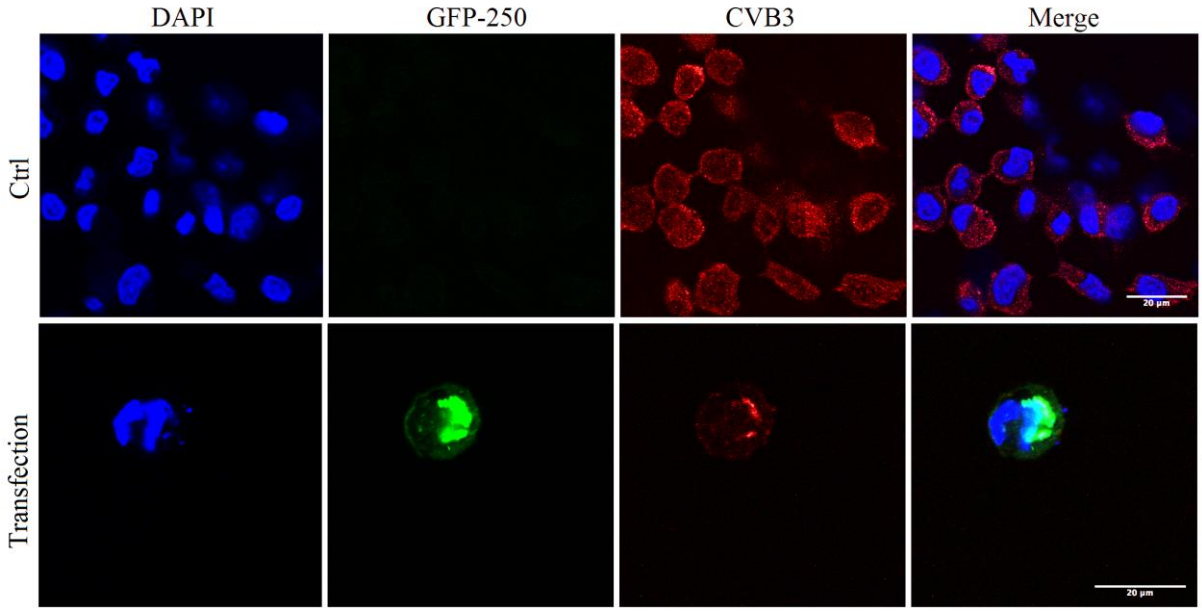

Figure 5. CVB3 infection of a GFP-250 –transfected cell. A549 cells were transfected with GFP-250 –plasmid for 48 hours, infected with CVB3 and fixed after 5h p.i. GFP-250 (green) resembles aggresomes. Infected cells were identified with virus capsid antibody (red). Cells were imaged with fluorescence confocal microscope. CVB3-infected GFP-250 positive cell is a representative of about 35 analysed cells of one experiment. Scale bars 20 µm.

As the capsid labeling left us unsure whether or not viruses were able to infect the cells, we wanted to study if viral replication had taken place by labeling viral replication intermediate dsRNA from GFP-250 transfected cells. Nontransfected but infected cells contained abundant viral double-stranded RNA right next to the nucleus, indicating normal viral replication. However, as with CVB3 capsids, viral RNA appeared unusual in transfected cells: Viral RNA colocalized with GFP-250, and the amount of RNA was very

low (Figure 6, indicated by arrows), suggesting that aggresomes might interfere with CVB3 replication as well. However, since we managed to induce only a few natural-looking aggresomes, and high expression levels of GFP-250 itself might be cytotoxic for cells, these results should be interpreted with caution.

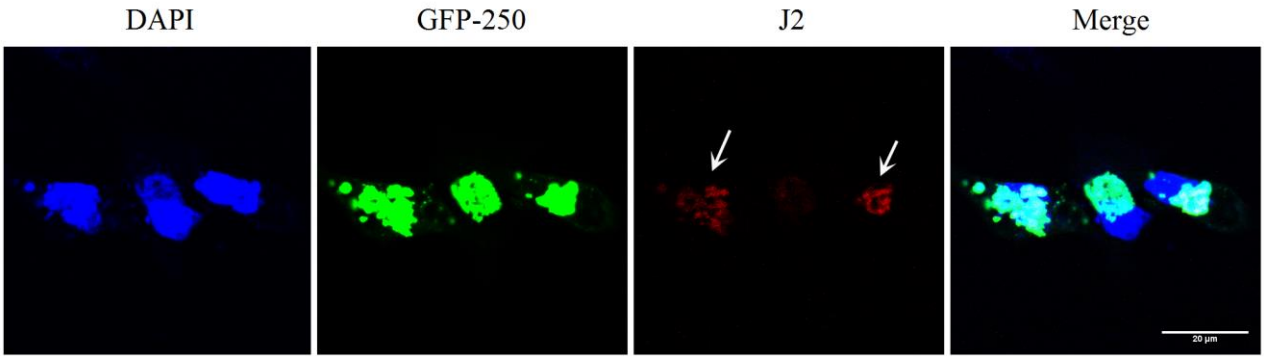

Figure 6. CVB3 infection of a GFP-250 –transfected cell. A549 cells were transfected with GFP-250 –plasmid for 48 hours, infected with CVB3 and fixed after 5h p.i. GFP-250 (green) resembles aggresomes. Infected cells were identified with virus double-stranded RNA antibody (red, indicated by arrows). Cells were imaged with fluorescence confocal microscope. CVB3-infected GFP-250 positive cells are representative of about 50 analysed cells of one experiment. Scale bar 20 µm.

4.2. Immunolabeling of aggresome-related proteins during CVB3 infection

Next, we decided to study the involvement of the activation of aggresomal pathway during CVB3 infection by labeling proteins that are known to be involved in aggresome formation: vimentin, γ-tubulin, TGN46 (in order to visualize the Golgi apparatus), calreticulin (to visualize ER) and Hsp70. By comparing changes in these proteins to the ones known to be induced in aggresome formation, we wanted to assess whether the aggresomal pathway could play a role in CVB3 infection. Since we knew from our earlier studies that a cage-like vimentin structure starts to form around 4 h p.i. during enterovirus infection (Turkki et al., unpublished data), A549 cells were infected with CVB3 for 5 h before fixation. Cells were immunolabeled with antibodies targeted to vimentin, γ-tubulin, TGN38, calreticulin and Hsp70, and imaged with fluorescence confocal microscope. Infected cells were identified by the fluorescent labeling of viral replication intermediate dsRNA and/or virus capsid.

4.2.1. **CVB3 infection induces a cage-like vimentin and the crescent shape of the nucleus**

Throughout this study, vimentin was normally found as an elongated network in the cytoplasm and around the nucleus in uninfected cells (Figure 7, Ctrl). CVB3 infection had a strong effect on vimentin structure: Normally highly elongated network seemed to have collapsed, which resulted in a packed structure in the perinuclear region (Figure 7, CVB3).

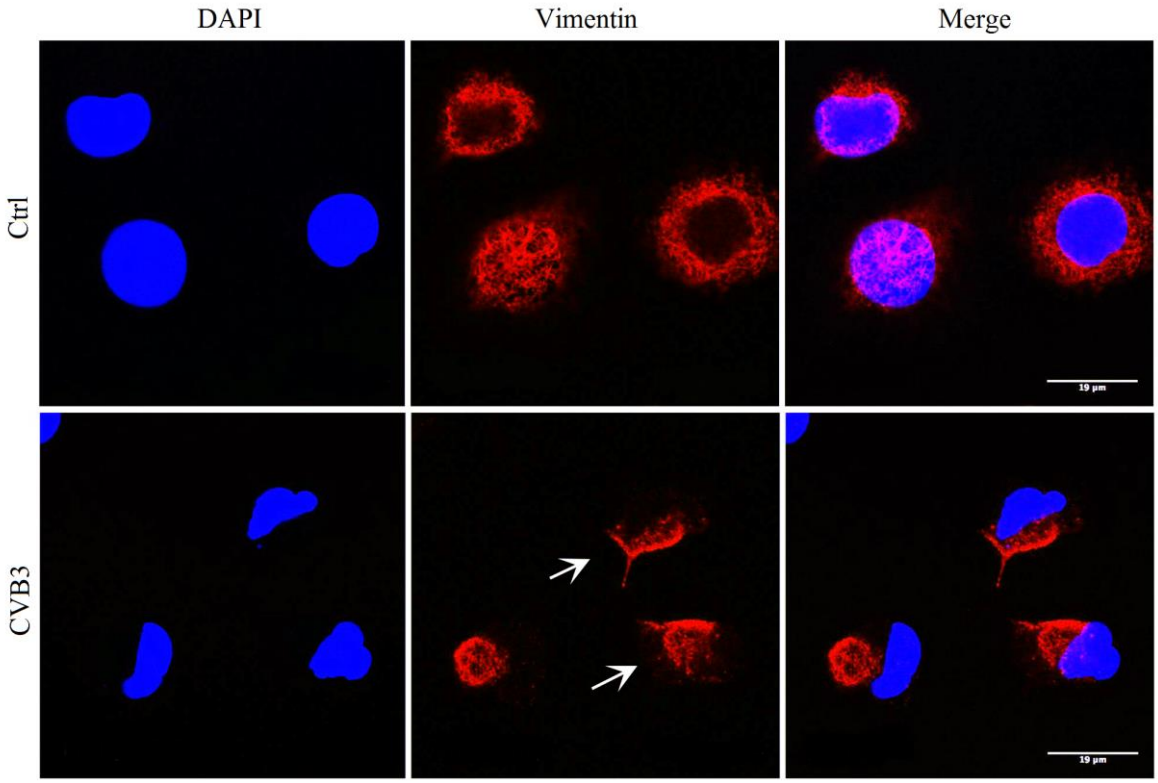

Figure 7. Vimentin network in control and CVB3 infected cells. A549 cells were infected with CVB3 and fixed after 5h p.i. Vimentin (red) was immunolabeled and cells were observed with fluorescence confocal microscope. Vimentin network often resulted in atypical vimentin, e.g. an asterisk-like structures (indicated by arrows). In addition, the nuclei of infected cells often showed the crescent shape. CVB3-induced vimentin structures are representative of six individual experiments, including at least 10 cells per each experiment. Infected cells are shown in lower panel (CVB3), uninfected in upper panel (Ctrl). Scale bars 19 µm.

Virus-induced vimentin structure resembled a cage-like complex that was located right next to the crescent shaped nucleus. This characteristic change in vimentin structure was induced in the majority of CVB3-infected cells: For example, in one experiment (including 114 cells), a cage-like vimentin was found in ~73% of infected cells, whereas in

uninfected cells this kind of rearrengement was barely ever seen (data not shown). If a vimentin-cage was not formed, infection still seemed to interfere with normal vimentin network and induce untypical structures, e.g. an asterisk-like structure (Figure 7, CVB3, indicated by arrows). In addition, it was observed that infection often caused the crescent shape of the nucleus throughout this study, indicating that together with a cage-like vimentin, this morphological change can be used as a reliable tool to identify CVB3-infected A549-cells.

4.2.2. γ-tubulin concentrates in the perinuclear region during CVB3 infection

γ-tubulin is commonly used to define the location of the MTOC in the cytoplasm, and aggresomes form around the MTOC (Johnston et al., 1998). γ-tubulin was largely diffused in the cytoplasm of uninfected cells (Figure 8A, Ctrl). A few highly concentrated spots right next to the nucleus were found (Figure 8A, Ctrl, indicated by an arrowhead), but the protein was mainly spread on a large area in the cytoplasm. It was clear that CVB3 infection altered γ-tubulin, as infected cells seemed to have highly concentrated γ-tubulin-foci (Figure 8A, CVB3, indicated by arrows). These particles were larger in size, and one cell usually contained several of them in the cytoplasm. These complexes were located around the nucleus or mainly in the perinuclear region, where a characteristic vimentin structure was also formed. In the perinuclear region, γ-tubulin was usually found at the edges or the inner part of vimentin structure, and this was not merely due to cell shrinkage as DIC-images showed that γ-tubulin was truly accumulated to the perinuclear region, while the cell boundaries were further away (Figure 8B).

Since it seemed that CVB3 infection altered γ-tubulin, and caused the formation of more concentrated γ-tubulin foci around the nucleus and in the perinuclear region, the quantification of the confocal images from one experiment was decided to be performed. The intensity of γ-tubulin signal and the number of γ-tubulin particles were quantified with Bioimage XD software (Figure 8C). Quantification results showed that both the number of γ-tubulin particles and the intensity of γ-tubulin per cell were significantly lower in CVB3-infected cells. The results were counted from only one experiment, including 14 CVB3-infected and 15 uninfected cells. In these results, we can see hints of statistical support for

our findings. However, to confirm quantification results in future, we need to perform experiments with more statistics.

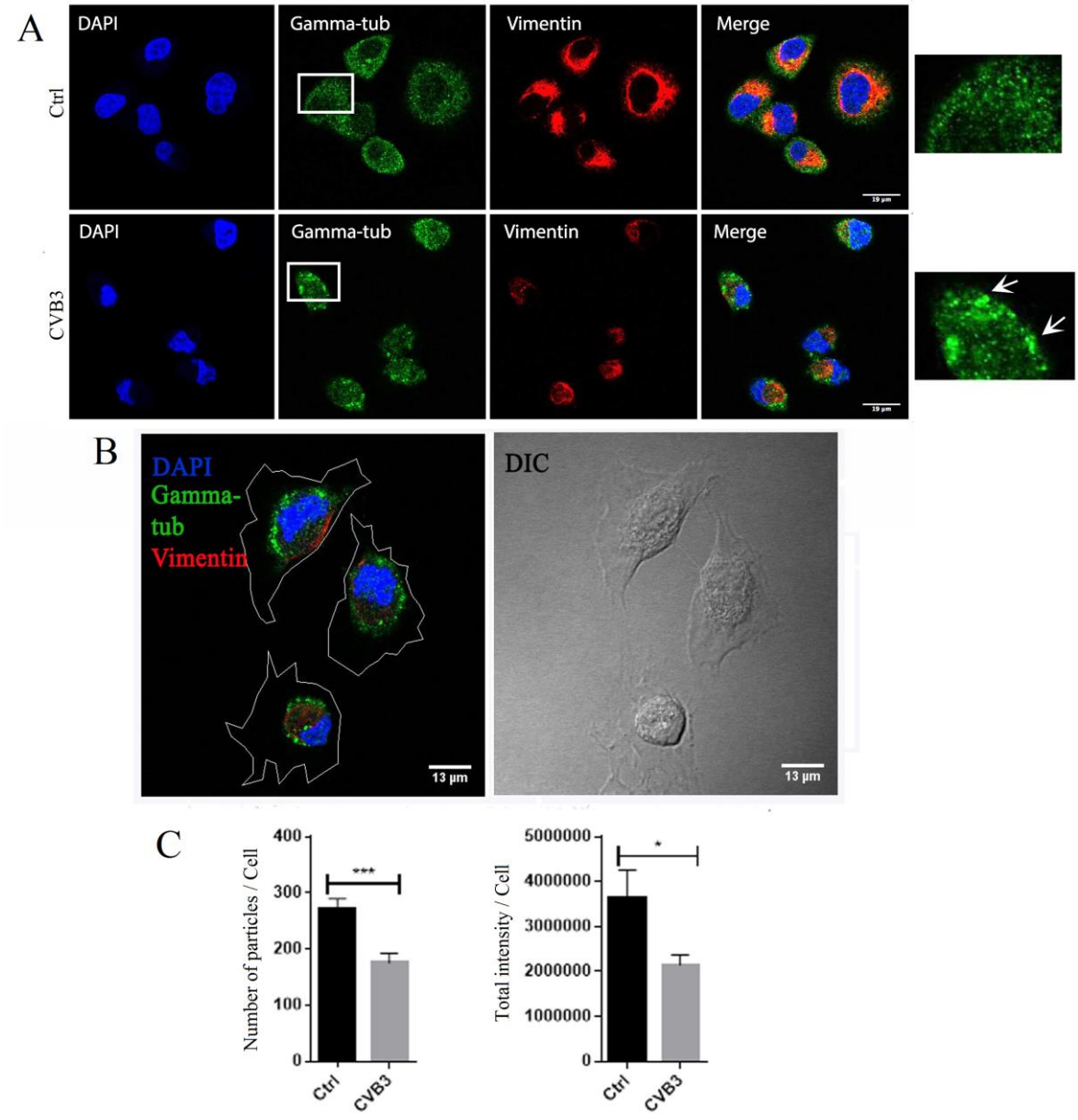

Figure 8. *γ*-tubulin (Gamma-tub) in CVB3 infection. A) A549 cells were infected with CVB3 and fixed after 5h p.i. *γ*-tubulin (green) and vimentin (red) were immunolabeled and cells were observed with fluorescence confocal microscope. Uninfected cells are shown in upper panel (Ctrl) and infected cells in lower panel (CVB3). Infected cells contained several highly concentrated *γ*-tubulin particles around the nucleus and in the perinuclear region (indicated by arrows). Results are representative of two individual experiments, including at least 15 cells per each. Scale bars 19 µm. B) Confocal images showing the outlines of CVB3-infected cells. In the left panel, *γ*-tubulin (green), vimentin (red) and the cell outlines are shown. DIC-image of cells is shown in the right panel (DIC). Scale bars 13 µm. C) Quantification analyses of *γ*-tubulin. The intensity of *γ*-tubulin signal and the number of *γ*-tubulin particles were quantified with Bioimage XD. The results were counted from one experiment, including about 15 cells per sample. *p = 0.0354, ***p = 0.0005.

4.2.3. **CVB3 infection disturbs the Golgi network and causes the accumulation of Golgi proteins in the perinuclear region**

The Golgi apparatus was identified by labeling TGN46, a trans-Golgi network marker. In uninfected cells, labeling of TGN38 showed one compact structure right next to the nucleus, indicating the location of the Golgi (Figure 9A, Ctrl). CVB3 infection had a considerable effect on Golgi-structure: Compact signal next to the nucleus was lost, but bright signal was seen in the perinuclear region, as if Golgi proteins had packed there with vimentin (Figure 9A, CVB3). Some of Golgi proteins were found around the crescend-shaped nucleus, but the majority of them formed a ball-like structure around vimentin. The cell outlines showed that Golgi proteins had accumulated in the perinuclear region, and this was not simply due to cell shrinkage (Figure 9, CVB3, Merge). The presence of Golgi signal in wider area might suggest the increased expression of trans-Golgi proteins or the degradation of the Golgi apparatus.

As it seemed that the Golgi might have degraded or the expression of Golgi proteins might have increased during CVB3 infection, we quantified the confocal images from one experiment. The intensity of Golgi signal was quantified by using Bioimage XD software (Figure 9B). According to results, the increased expression of Golgi proteins is supported, as the increased intensity during CVB3 infection was statistically significant. However, this quantification result was counted only from one experiment, including about 12 CVB3-infected and uninfected cells. To confirm this result, we need to repeat quantification analysis to get more statistical support.

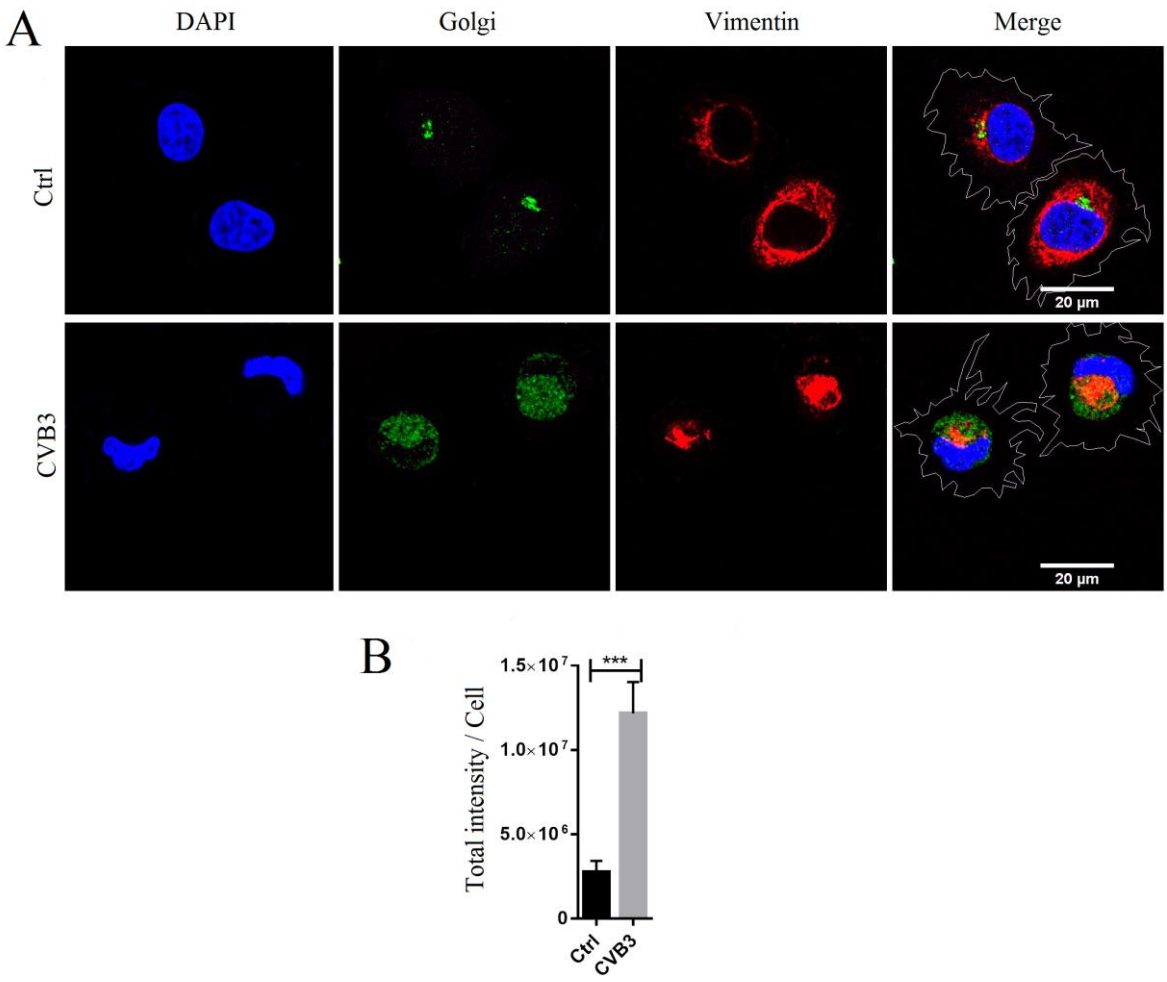

Figure 9. A) The Golgi apparatus in control and CVB3 infected cells. A549 cells were infected with CVB3 and fixed after 5h p.i. The Golgi (green) and vimentin (red) were immunolabeled in CVB3-infected cells (CVB3, the lower panel) and uninfected (Ctrl, the upper panel) cells and observed with fluorescence confocal microscope. The outlines of cells are shown in Merge-images. Infected cells are representative of one experiment, including approximately 30 observed cells. Scale bars 20 µm. B) Quantification analysis of Golgi proteins. The intensity of Golgi protein signal was quantified with Bioimage XD. Quantification result was counted from one experiment, including about 12 CVB3-infected and uninfected cells. ***p = 0.0002.

4.2.4. **The ER wraps around the nucleus and forms a ball-like structure in the perinuclear region in CVB3 infection**

In our experiments, the ER was identified by using an antibody specific to calreticulin. In uninfected cells, ER formed large and highly diffuse network in the cytoplasm, as expected (Figure 10, Ctrl). Changes in the ER were clearly seen in infected cells: Normally widely distributed membrane structures formed a highly packed ER complex in the perinuclear region with a cage-like vimentin structure, as if vimentin structure was enclosed by the ER (Figure 10, CVB3). In addition to a ball-like structure in the perinuclear region, the ER formed a thin layer around the nucleus. The outlines of cells confirmed the clear packaging of ER to the perinuclear region, which was not caused by the cell shrinkage (Figure 10, CVB3, Merge). Altogether, it seems that CVB3 infection leads to drastic alterations to the ER membranes. Whether this contributes to ER stress should be studied in more detail.

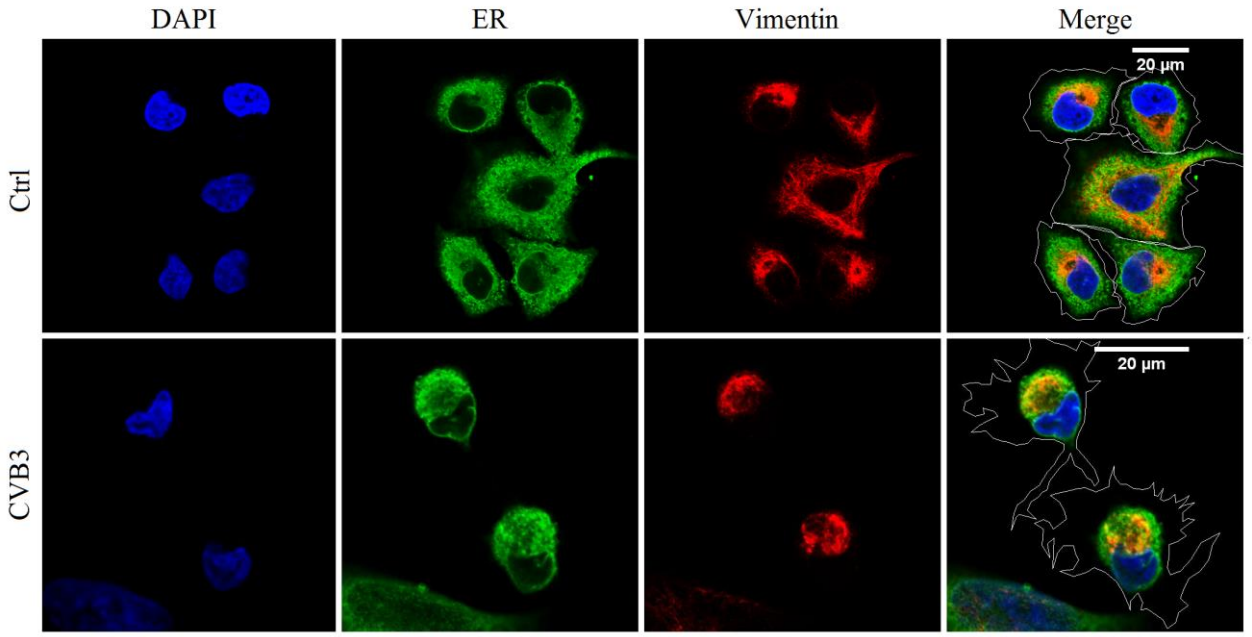

Figure 10. The formation of a ball-like ER structure in CVB3 infection. A) A549 cells were infected with CVB3 and fixed after 5h p.i. ER (green) and vimentin (red) were immunolabeled in CVB3-infected (CVB3, the lower panel) and uninfected (Ctrl, the upper panel) cells, which were then analysed with fluorescence confocal microscope. The outlines of cells are shown in the Merge-images. Results are representative of one experiment, including about 130 analysed cells. Scale bars 20 µm.

4.2.5. **Hsp70 accumulates in the nucleus and perinuclear region in CVB3 infection**

In this study, we found that uninfected cells expressed Hsp70 mainly in the cytoplasm and nucleus as highly concentrated spots (Figure 11A, Ctrl). The overall expression seemed to be quite low in uninfected cells. CVB3 infection caused Hsp70 to form even more highly concentrated complexes mainly in the nucleus (Figure 11A, CVB3, indicated by arrows). Although the majority of the protein had accumulated in the nucleus, some Hsp70 was found concentrated in the perinuclear region, most probably due to translocation from the rest of the cytoplasm since diffuse Hsp70 staining seemed diminished.

Since we saw differences between the expression and location of Hsp70 in CVB3-infected and uninfected cells, we wanted to be certain about the result and quantitate the confocal images. The intensity of Hsp70 signal and the colocalization with DAPI were quantified with Bioimage XD software (Figure 11C). Results for the intensity of Hsp70 were counted from three different experiments, and the colocalization from two, including 10-20 cells per each experiment. Quantification results showed that the intensity of Hsp70 protein was decreased in CVB3 infected cells, suggesting that the amount of Hsp70 does not increase during CVB3 infection. Colocalization analysis showed that the increased colocalization of Hsp70 with DAPI during CVB3 infection was not statistically significant. To get more statistical significance in order to support translocation of Hsp70 from the cytoplasm to the nucleus, more experiments should be included to the colocalization analysis.

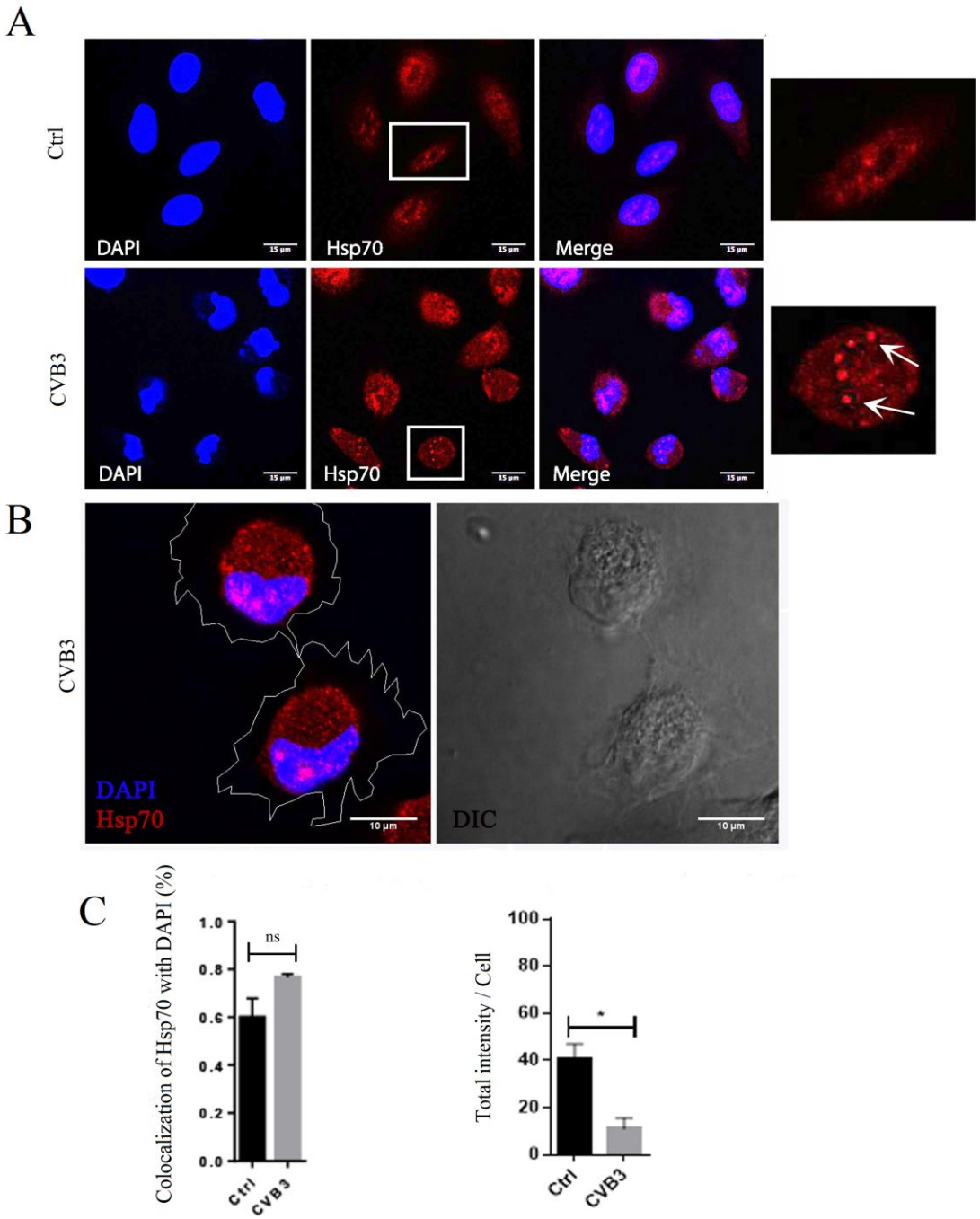

Figure 11. The accumulation of Hsp70 in the nucleus and perinuclear region in CVB3 infection. A) A549 cells were infected with CVB3 and fixed after 5h p.i. Hsp70 (red) was immunolabeled in CVB3-infected (CVB3, the lower panel) and uninfected control cells (Ctrl, the upper panel). Cells were then analysed with fluorescence confocal microscope. Results are representative of three experiments, including 10-30 analysed cells per each experiment. Scale bars 15 µm. B) Confocal images showing the outlines of CVB3-infected cells. In the left panel (Merge), Hsp70 (red) and the cell outlines are shown. DIC-image of cells is shown in the right panel (DIC). Scale bars 10µm. C) Quantification analysis of Hsp70. The intensity of Hsp70 signal and the colocalization of Hsp70 with DAPI were quantified with Bioimage XD. The results of the intensity of Hsp70 were counted from three different experiments, and the colocalization with DAPI from two, including about 10-20 cells per each experiment. *p = 0.0196.

4.2.6. **Ubiquitin is present in the perinuclear region in CVB3 infection**

In uninfected cells, ubiquitin was mainly evenly distributed both in the nucleus and cytoplasm, although some concentrated spots were found (Figure 12A, Ctrl). As with the most of other studied proteins in our experiments, CVB3 infection also caused the movement of ubiquitin to the perinuclear region (Figure 12A, CVB3). To confirm that this ubiquitin translocation was not due to cell shrinkage, DIC-images were taken and the outlines of cells were drawn (Figure 12A, CVB3, Merge). Ubiquitin from the nucleus had possibly moved to the perinuclear region, as the amount of protein in the nucleus seemed to be low compared to uninfected cells.

As free ubiquitin seemed to be recruited to the perinuclear region, we wanted to quantitate the confocal images with BioImage XD software (Figure 12B). The recruitment of free ubiquitin to smaller areas could be seen as the decreased number of ubiquitin particles. Results were counted from three different experiments, including 10-20 cells per each. Quantification results showed that the number of ubiquitin particles was significantly lower in CVB3-infected cells, which supports the accumulation of ubiquitin to the perinuclear region.

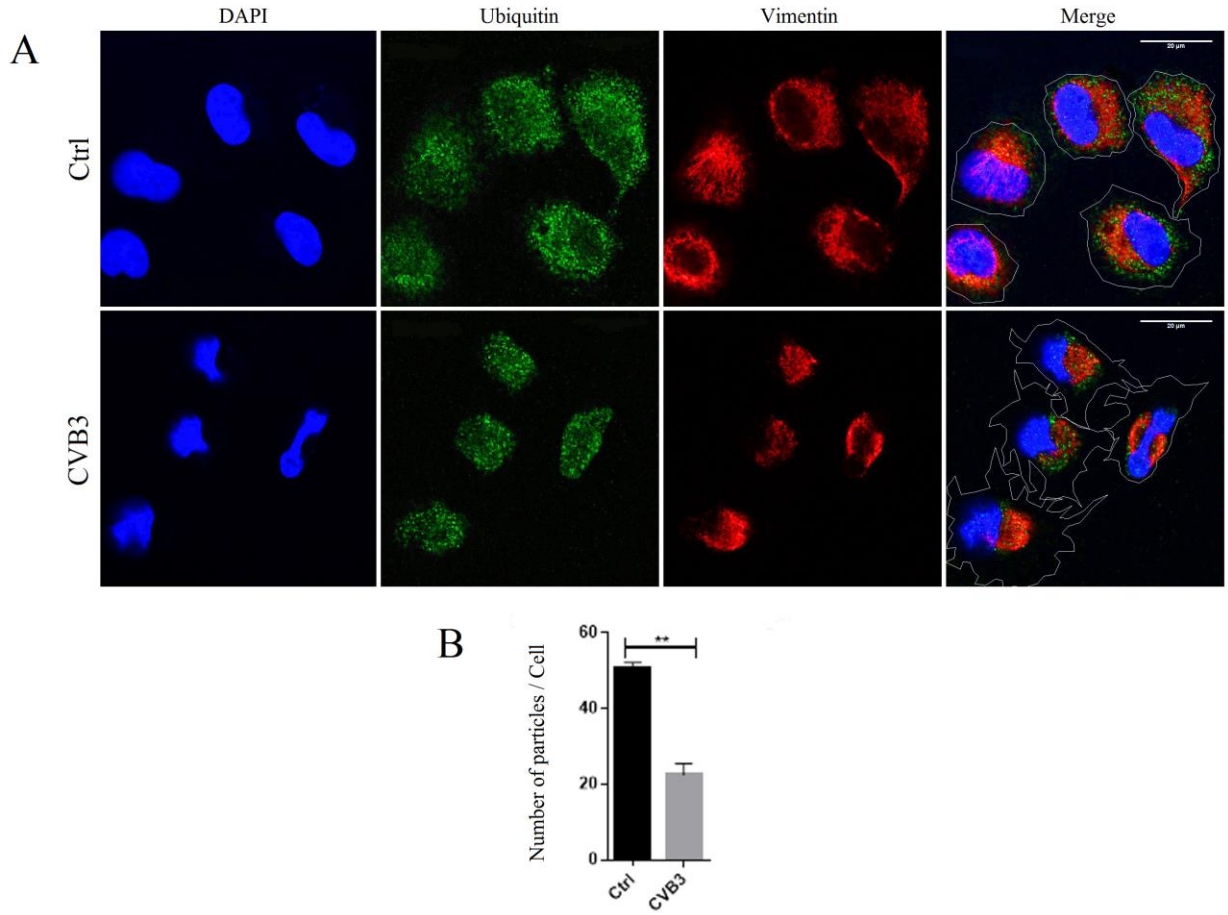

Figure 12. The recruitment of ubiquitin from the nucleus and cytoplasm to the perinuclear region in CVB3 infection. A) A549 cells were infected with CVB3 and fixed after 5h p.i. Ubiquitin (green) and vimentin (red) were immunolabeled in CVB3-infected (CVB3, the lower panel) and in uninfected (Ctrl, the upper panel) cells and imaged with fluorescence confocal microscope. Merge-images show the outlines of cells. Results are representative of four experiments, including 15-45 analysed cells per each experiment. Scale bars 20 µm. B) Quantification analysis of ubiquitin. The number of ubiquitin particles in CVB3-infected and uninfected cells was quantified with Bioimage XD. The results were counted from three different experiments, including about 10-20 cells per each experiment. **p = 0.0039.

4.3. Microtubules are involved in the formation of a cage-like vimentin structure

To study the role of microtubules in CVB3 infection, we performed an assay in which we treated CVB3-infected A549 cells with 33 µM nocodazole. Drug was added either together with the virus or 1, 3, or 5 h p.i., and cells were fixed after 6 h p.i., respectively. Cells were then immunolabeled with vimentin and CVB3 capsid–antibodies, and imaged with fluorescence confocal microscope. Infected cells were indentified by the labeling of viral capsids and the morphological change of the nucleus.

It was noticed that nocodazole affected virus-induced vimentin structures. Only minor changes were observed when the drug was added 5 h p.i., when the vimentin structures have usually already taken their cage-like form, but we observed notable effects when nocodazole was administered 3 h p.i. (Figure 13). Effects of nocodazole were diverse: In many cells, the expression levels of vimentin were extremely low (Figure 13A. B), and in some cases, vimentin seemed to be in monomeric form. Quite often, vimentin only surrounded the nucleus, instead of forming a perinuclear structure (Figure 13A. B). Some cage-like structures were found, but they tended to differ from common virus-induced structures in their location and shape. These atypical structures seemed not to be as tight (Figure 13A. C), and they were often located in another end of the nucleus, rather than in the perinuclear region next to the nucleus. In fact, some structures did not resemble a cage at all (Figure 13A. D, E and F, indicated by an arrow).

According to visual observation, nocodazole treatment seemed to have the strongest effects on vimentin when the drug was administered simultaneously with the virus or 1 h p.i.. To study the effects of nocodazole on CVB3-induced vimentin structures in more detail, we counted the percentage of infected cells having atypical vimentin structures (Figure 13B.). Results were counted from one experiment, including 113-125 cells per each sample. Indeed, it was seen that about 80% of infected cells that were treated with nocodazole simultaneously with the virus, showed vimentin structures that differed from a characteristic, cage-like vimentin. When administered 1 h and 3 h p.i., nocodazole still notably caused unusual vimentin structures but the effect was descenting, suggesting that microtubules are involved in the formation of a cage-like vimentin in the early phase of CVB3 infection. In addition, drug treatment at 5 h p.i. did not have statistically significant difference in the amount of cells having atypical vimentin structures, indicating the role in the early formation of a cage-like vimentin, not in the maintenance of this structure. To evaluate the possible changes in CVB3 infection efficiency induced by nocodazole, we counted the infection percentage of nocodazole-treated CVB3-infected cells (Figure 13C). Results were counted from one experiment, including 200-240 cells per sample. Statistical analysis showed that there were no significant differences in percentages between the virus control and drug-treated, infected cells.

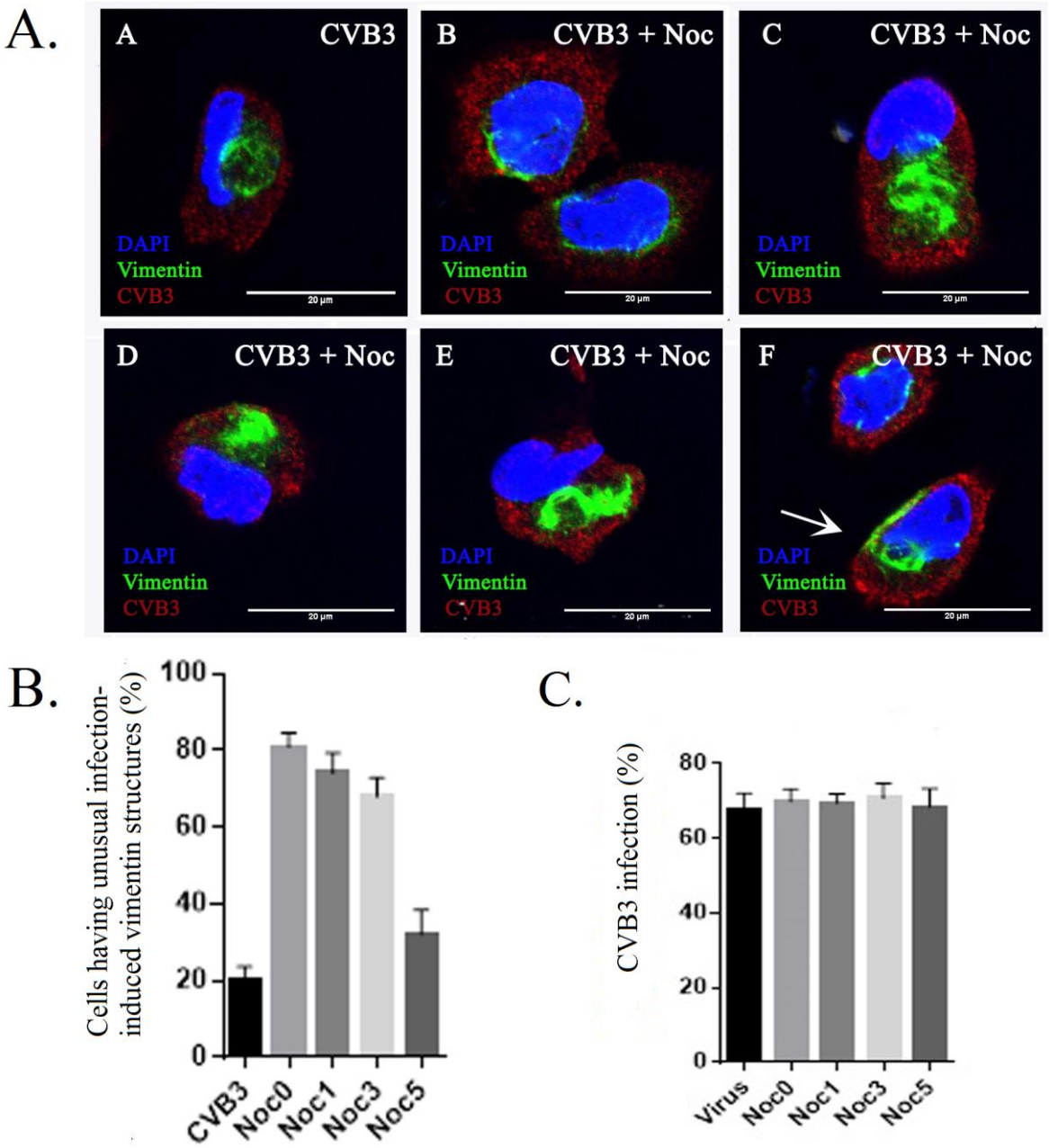

Figure 13. A. 3 h p.i. Nocodazole treatment of CVB3-infected A549 cells, resulting in diverse drug-affected, atypical virus-induced vimentin structures. Nocodazole was added to infected cells at 3 h p.i., and left until the cells were fixed at 6 h p.i. Cells were labeled CVB3 and vimentin antibodies and imaged with fluorescence confocal microscope. Nocodazole treatments in which the drug was added 0 and 1 h p.i. caused same kinds of vimentin structures. Nocodazole treatment resulted in several kinds of infection-induced vimentin structures (B, C, D, E, F; CVB3 + Noc) which differ from usual cage-like structure formed in CVB3 infection (A, CVB3). Scale bars 20 µm. B. The percentage of CVB3-infected cells having unusual virus-induced vimentin structures was counted. The differences between the control (CVB3) and Noc 0, Noc 1 and Noc 3 h p.i. are statistically significant (****$p < 0.0001$), but insignificant between the control and Noc 5 h p.i.. The results were counted from one experiment, including 113-125 cells per sample. C. Infection percentage of nocodazole –treated CVB3-infected cells was counted. All the differences between the virus control and each drug-treated sample were statistically insignificant. The results were counted from one experiment, including 200-240 cells per sample.

5. Discussion

Aggresome formation is a cellular stress reaction in which several changes in cellular structures and proteins occur (For a review, see Kopito, 2000). These changes include the redistribution of vimentin filaments, which results in a cage-like structure surrounding the MTOC in the perinuclear region. In addition, the Golgi apparatus is displaced and several proteins, including Hsp70 and ubiquitin, are recruited to the perinuclear region. It has been recently observed that human enterovirus infection alters vimentin dynamics and induces the formation of a cage-like structure in the perinuclear region (Turkki et al., unpublished data), which highly resembles the one induced during aggresome formation. Due to this resemblance, we wanted to study the possible activation of aggresomal pathway during CVB3 infection. Throughout this study, we confirmed that CVB3 infection causes the formation of a cage-like vimentin structure, similar to one reported in aggresome formation. As the vimentin rearrangements seemed to be induced in the majority of infected cells throughout our experiments, together with the crescent shaped nucleus, we were able to use this cage-like vimentin structure as a tool for identifying CVB3-infected A549 cells.

We also demonstrated that CVB3 infection disturbs the structure of Golgi apparatus and causes the recruitment of Hsp70 and ubiquitin to the perinuclear region, which all support the role of aggresomal pathway in CVB3 infection. Golgi apparatus had clearly spread from a distinct small aggregate located next to the nucleus to a larger area in the perinuclear region, which could indicate degradation, or even vesiculation of the Golgi apparatus during infection. The degradation of the Golgi resembles the displacement of Golgi induced by proteasome inhibitor MG132 in SH-SY5Y and HeLa cells (Diaz-Corrales et al., 2012; Wojcik et al., 2004), indicating that CVB3 infection does lead to changes resembling the ones occurring during aggresome formation. However, to confirm the possible degradation of the Golgi apparatus, antibodies against Golgi stack structures and other compartments in addition to TGN should be used in future. As changes in the Golgi structure may cause the disruption of normal membrane traffick, it might be possible that CVB3-induced fragmentation of TGN can also disturb the normal membrane traffic from the TGN to other destinations. This could be experimentally analysed in future. Although it has been demonstrated that ER to Golgi transport is not normally inhibited by aggresome formation (Garcia-Mata et al. 1999; Diaz-Corrales et al. 2012), MG132-

mediated induction of aggresomes causes the fragmentation of TGN in SH-SY5Y and disturbs the normal traffick from the Golgi to the plasma membrane (Diaz-Corrales et al., 2012).

Our studies demonstrated clear Hsp70 accumulation into the nucleus and perinuclear region during CVB3 infection, which might support the activation of aggresomal pathway where Hsp70 has been previously shown to aggregate in the perinuclear region (Wigley et al., 1999; Garcia-Mata et al., 1999). However, as stressful conditions can also induce the translocation of Hsp70 from the cytoplasm to the nucleus (Welch and Feramisco, 1984), the results also support the activation of cellular stress responses during infection. Despite the clear changes that were visually observed from confocal images, our quantification result showing the increased colocalization of Hsp70 with the nucleus in infected cells was not statistically significant. However, as the sample size was only moderate in all of the quantifications done in this thesis, these results should not be used to make too far assumptions. Upregulation of Hsp70 protein expression has been connected to at least PRRS, West Nile, and few plant virus infections (Gao et al., 2014; Pastorino et al., 2009; For a review, see Nagy et al., 2011), but this seems not to be the case with CVB3 as indicated by the confocal images. Hsp70 proteins are crucial part in both normal cellular function and the recovery from stressful conditions, as they facilitate several events related to proteins: folding and refolding, the prevention of aggregation and degradation of unstable or misfolded proteins, and transport between cellular compartments (For a review, see Daugaard et al., 2007). Members of the Hsp70 family have been shown to have an effect on Hepatitis C replication and the release of viral particles via the interaction with replication proteins (Chen et al., 2010). In addition, the interaction of Hsp70 with the capsid precursor protein of poliovirus and Coxsackievirus B1 has also been shown, which suggests the role of Hsp70 in enterovirus assembly (Macejak and Sarnow, 1992).

Ubiquitination is commonly related to the aggresome formation, although it is not involved in the formation of artificially formed aggresomes by GFP-250, SOD or ATP7B (Garcia-Mata et al., 1999; Johnston et al., 2000). In our experiments, CVB3 infection caused substantial relocation of ubiquitin to the perinuclear region, suggesting the activation of aggresomal pathway in which ubiquitin is involved. The recruitment of ubiquitin particles from large area in the cytoplasm to the perinuclear region was supported by our preliminary quantification analysis that showed the decreased number of ubiquitin particles

in CVB3-infected cells. Although the quantification analysis needs to be repeated to confirm the accumulation of ubiquitin to smaller areas, our results suggest the involvement of ubiquitin in CVB3 infection. Ubiquitin has a role in many cellular processes, like autophagy, protein sorting and proteasome-mediated degradation, and the ubiquitination of a protein often forms a signal for it's degradation via proteasome system (For a review, see Shaid et al., 2013). Thus, apart from the activation of aggresomal pathway, the host cell might identify viral proteins as harmful, leading to the ubiquitination of viral particles and their degradation. Indeed, via regulation of the type I interferon expression, ubiquitination is one important factor in innate immune responses against viral infection (For a review, see Heaton et al., 2016). In addition to the usage of ubiquitin as a cellular defence mechanism, ubiquitin can also be exploited by the virus as recently shown with Influenza A virus (Banerjee et al., 2014). By utilizing ubiquitin modification system of the host cell, viruses can possibly reduce interferon production and attenuate innate immunity. Suggested methods of manipulating ubiquitination used by viruses are, for example, hijacking and the viral expression of the host ubiquitin enzymes, including deubiquitination and E3-ligation enzymes, from which the latter is one of the three enzymes involved in the covalent attachment –process of ubiquitin (For a review, see Shaid et al., 2013).

In our experiments, CVB3 infection did not cause the formation of one large γ-tubulin aggregate that clearly defines the location of the MTOC inside a vimentin cage, as would be expected during aggresome formation. Despite this, γ-tubulin had clearly accumulated to the perinuclear region, which was also supported by our preliminary quantification analysis of confocal images. The aggregation of γ-tubulin in HeLa and SH-SY5Y cells, induced by proteasome inhibitors, occurs after 16 h and 24 h (Diaz-Corrales et al., 2012; Didier et al., 2008). Thus, it may be possible that 5 h is not enough for the formation of a single γ-tubulin complex in CVB3-infected cells. However, during aggresome formation, several components are recruited to the perinuclear region around the MTOC, meaning that the formation of a large γ-tubulin aggregate should presumably be one of the first events occurring after the initiation of aggresomal pathway. According to our preliminary quantification results, the total intensity of γ-tubulin signal was shown to be significantly lower, possibly indicating the decreased amount of γ-tubulin during CVB3 infection. In the study by Didier et al. (2008), proteasomal inhibition in HeLa cells seemed to increase the

amount of γ-tubulin, but immunoblot experiments showed that the levels of γ-tubulin were not increased.

Intriguingly, in addition to vimentin, the ER was also found to form a ball-like structure in the perinuclear region during CVB3 infection. This clear moprhological change seemed to occur in the majority of CVB3-infected cells, together with the collapse of vimentin. According to our confocal images, highly packed ER complex seemed to surround a cage-like vimentin. The aggresome formation by bortezomib in pancreatic cancer cells has been shown to induce a similar ER structure in the perinuclear region (Nawrocki et al., 2006). Interestingly, our CVB3-induced ER structures, however, looked more compact than the one induced by bortezomib. Another cellular stress event where the ER is involved is ER stress, in which unfolded or misfolded proteins become aggregated in the ER, which triggers the UPR. Many viruses, including CVB3, have been shown to modulate components of the ER stress signaling pathway (For a review, see He, 2006; Zhang et al., 2010). As the activation of ER stress has been previously studied in HeLa and cardiomyocyte –cells by Zhang et al., changes in the structure of ER during CVB3 infection were not unexpected. As strong alterations to the ER structure could potentially lead to or be a consequence of ER stress, our results also indicated the involvement of ER stress. However, well-known structural response to ER stress has been demonstrated to be the expansion of the ER, resulting in approximately the five-fold increased volume of the lumen (For a review, see Schonthal, 2012). For example, the induction of ER stress response by cyclosporine A in HeLa cells causes the vesiculation, and thus the expansion of the ER (Ram and Ramakrishna, 2014). Interestingly, our results suggest that CVB3 infection results in the collapsed ER, rather than in expanded structure. Indeed, further experiments have shown that important components of the ER stress signaling pathway are not modulated during CVB3 infection (Turkki et al., unpublished data). Although the activation of ER stress response does not seem to be involved in CVB3 infection, our results indicate that the ER is clearly altered by virus. Another human enterovirus, poliovirus, exploits ER membranes by forming replication complexes in the ER (Rust et al., 2001). Thus, changes in the structure of ER during CVB3 infection may be a consequence of similar exploitation of ER membranes. It is also possible that the formation of a ball-like ER structure is induced as a secondary effect of the interaction between the ER and vimentin. Due to the interaction, collapsing vimentin filaments may “drag” the

surrounding ER structures into the perinuclear region. In that case, ball-like ER may act as a supporting scaffold during viral replication and assembly together with vimentin cage, which has been suggested to happen in Dengue virus infection (Lei et al., 2013).

Despite the challenges in aggresome formation by GFP-250 transfection, we did manage to analyse few of the cells with artificially induced aggresomes. These indicated that simultaneous CVB3 infection and aggresome formation resulted in inhibited CVB3 infection, suggesting that CVB3 might use the same cellular mechanisms that are involved in aggresomal pathway. However, despite this interesting result, it has to be interpreted with caution because this observation was based on only few viable cells. Alternatively, another methods to induce aggresomes could be used, such as the overexpression of SOD, ATP7B or CFTR (Johnston et al., 1998; Harada et al., 2001; Johnston et al., 2000). Furthermore, several proteasome inhibitors, including MG132, ZL3H and lactacystin, can also trigger aggresome formation (Johnston et al., 1998; Ward et al., 1995). As aggregated proteins are actively transported from the cytoplasm to the MTOC along microtubules during aggresome formation, we studied the role of vimentin cages and possible aggresomal activation by microtubule depolymerization. Nocodazole treatment has been demonstrated to inhibit aggresome formation by leaving protein aggregates distributed in the cytoplasm (Johnston et al., 1998). Furthermore, the transport of vimentin aggregates depends on microtubules (Prahlad et al., 1998). Our results indicated that vimentin structure formation was dependent on intact microtubule network, but microtubule network was not involved in the maintenance of these vimentin structures, as nocodazole did not have a noticeable effect at 5 h p.i., when vimentin had already taken it’s cage-like form.

Vimentin collapse to the perinuclear region has also been shown to be induced by other viruses, at least Frog virus 3, Vaccinia and ASFV (Stefanovic et al., 2005; Murti and Goorha, 1983; Risco et al., 2002). However, the exact role of a cage-like vimentin structure during viral infection is currently unknown, but it has been speculated that it may form a supporting scaffold for the viral factories. This assumption is based on the fact that quite often they concentrate viral proteins and/or replication factors, which is seen with ASFV and Vaccinia virus (Stefanovic et al., 2005; Risco et al., 2002). Similarly, also the replication intermediate dsRNA of CVB3 resides within these structures (Turkki et al., unpublished data). If vimentin-cage acts as a supporting scaffold during viral replication and assembly, nocodazole-induced untypical vimentin cages may fail in concentrating viral

particles, resulting in inefficient or abnormal CVB3 infection. However, in our studies, the infection percentage was not affected by nocodazole treatment, which is consistent with the study showing the same result about the infection of another human enterovirus, Coxsackievirus A9 (Huttunen et al., 2014). Alternatively, vimentin structures may reduce infection by enclosing viral material and thus prevent the spread of viral proteins in the cytoplasm. Thus, these structures might act as a general cytoprotective response, resulting in the reduced viral assembly. In future, the roles of vimentin cages and the aggresomal activation should be evaluated by another methods, e.g. determining whether nocodazole treatment causes changes in the amount of CVB3 capsid proteins, which would reveal the effects of aggresomal components on viral production.

Taken together, CVB3 induces changes in key components involved in the aggresome formation, suggesting that activation of aggresomal pathway might take place during CVB3 infection. Here, we confirm that CVB3 infection induces a cage-like vimentin in the perinuclear region, a characteristic structural change occurring during aggresome formation. In addition, ubiquitin and Hsp70 are recruited to the perinuclear region, and the structure of the ER and Golgi are strongly altered. Although γ-tubulin does not form a large aggregate in the perinuclear region, CVB3 infection clearly induces changes in the distribution of γ-tubulin. Alterations in the structure of ER might support the "scaffolding" functions of ER during CVB3 infection. Several viruses, including Influenza A, have been suggested to take advantage of aggresomal machinery during viral processes. However, this machinery has not been previously associated with enteroviral infections. Thus, our results may give new information about the role of aggresomal pathway in enterovirus infection and the interactions between the host cell and virus. To further study the similarity between changes occurring in enterovirus infection and aggresome formation, proper aggresomes need to be induced by using other methods in future. To evaluate whether they are cytoprotective or favourable to virus, the effects of aggresome formation on viral infection should be observed. Additionally, the roles of single components of the aggresomal pathway, e.g. ubiquitination and heat shock proteins, should also be studied in more detail.

References

Abzug, M.J. 2014. The enteroviruses: Problems in need of treatments. *J.Infect.* 68, Supplement 1:S108-S114.

Banerjee, I., Y. Miyake, S.P. Nobs, C. Schneider, P. Horvath, M. Kopf, P. Matthias, A. Helenius, and Y. Yamauchi. 2014. Influenza A virus uses the aggresome processing machinery for host cell entry. *Science.* 346:473-477.

Bergelson, J.M., J.A. Cunningham, G. Droguett, E.A. Kurt-Jones, A. Krithivas, J.S. Hong, M.S. Horwitz, R.L. Crowell, and R.W. Finberg. 1997. Isolation of a common receptor for Coxsackie B viruses and adenoviruses 2 and 5. *Science.* 275:1320-1323.

Bergelson, J.M., J.G. Mohanty, R.L. Crowell, N.F. St John, D.M. Lublin, and R.W. Finberg. 1995. Coxsackievirus B3 adapted to growth in RD cells binds to decay-accelerating factor (CD55). *J.Virol.* 69:1903-1906.

Byun, Y., F. Chen, R. Chang, M. Trivedi, K.J. Green, and V.L. Cryns. 2001. Caspase cleavage of vimentin disrupts intermediate filaments and promotes apoptosis. *Cell Death Differ.* 8:443-450.

Chau, D.H., J. Yuan, H. Zhang, P. Cheung, T. Lim, Z. Liu, A. Sall, and D. Yang. 2007. Coxsackievirus B3 proteases 2A and 3C induce apoptotic cell death through mitochondrial injury and cleavage of eIF4GI but not DAP5/p97/NAT1. *Apoptosis.* 12:513-524.

Chen, Y.J., Y.H. Chen, L.P. Chow, Y.H. Tsai, P.H. Chen, C.Y. Huang, W.T. Chen, and L.H. Hwang. 2010. Heat shock protein 72 is associated with the hepatitis C virus replicase complex and enhances viral RNA replication. *J.Biol.Chem.* 285:28183-28190.

Cherry, J., and P. Krogstad. 2010. Enterovirus and Parechovirus infections. *In* Infectious Diseases of the Fetus and Newborn. WilsonnCB, V. Nizet, J. Remington, Y. O Klein and Y. Maldonado, editors. Elsevier Health Sciences, Philadelphia, US. 757.

Cheung, P.K., J. Yuan, H.M. Zhang, D. Chau, B. Yanagawa, A. Suarez, B. McManus, and D. Yang. 2005. Specific interactions of mouse organ proteins with the 5'untranslated region of coxsackievirus B3: potential determinants of viral tissue tropism. *J.Med.Virol.* 77:414-424.

Cordo, S.M., and N.A. Candurra. 2003. Intermediate filament integrity is required for Junin virus replication. *Virus Res.* 97:47-55.

Coyne, C.B., and J.M. Bergelson. 2006. Virus-induced Abl and Fyn kinase signals permit coxsackievirus entry through epithelial tight junctions. *Cell.* 124:119-131.

Daugaard, M., M. Rohde, and M. Jaattela. 2007. The heat shock protein 70 family: Highly homologous proteins with overlapping and distinct functions. *FEBS Lett.* 581:3702-3710.

Dave, J.M., and K.J. Bayless. 2014. Vimentin as an integral regulator of cell adhesion and endothelial sprouting. *Microcirculation.* 21:333-344.

Diaz-Corrales, F.J., I. Miyazaki, M. Asanuma, D. Ruano, and R.M. Rios. 2012. Centrosomal aggregates and Golgi fragmentation disrupt vesicular trafficking of DAT. *Neurobiol.Aging.* 33:2462-2477.

Didier, C., A. Merdes, J.E. Gairin, and N. Jabrane-Ferrat. 2008. Inhibition of proteasome activity impairs centrosome-dependent microtubule nucleation and organization. *Mol.Biol.Cell.* 19:1220-1229.

Du, N., H. Cong, H. Tian, H. Zhang, W. Zhang, L. Song, and P. Tien. 2014. Cell surface vimentin is an attachment receptor for enterovirus 71. *J.Virol.* 88:5816-5833.

El-Hage, N., and G. Luo. 2003. Replication of hepatitis C virus RNA occurs in a membrane-bound replication complex containing nonstructural viral proteins and RNA. *J.Gen.Virol.* 84:2761-2769.

Gao, J., S. Xiao, X. Liu, L. Wang, Q. Ji, D. Mo, and Y. Chen. 2014. Inhibition of HSP70 reduces porcine reproductive and respiratory syndrome virus replication in vitro. *BMC Microbiol.* 14:64-2180-14-64.

Garcia-Mata, R., Z. Bebok, E.J. Sorscher, and E.S. Sztul. 1999. Characterization and dynamics of aggresome formation by a cytosolic GFP-chimera. *J.Cell Biol.* 146:1239-1254.

Garcia-Mata, R., Y.S. Gao, and E. Sztul. 2002. Hassles with taking out the garbage: aggravating aggresomes. *Traffic.* 3:388-396.

Garmaroudi, F.S., D. Marchant, R. Hendry, H. Luo, D. Yang, X. Ye, J. Shi, and B.M. McManus. 2015. Coxsackievirus B3 replication and pathogenesis. *Future Microbiol.* 10:629-653.

Goldie, K.N., T. Wedig, A.K. Mitra, U. Aebi, H. Herrmann, and A. Hoenger. 2007. Dissecting the 3-D structure of vimentin intermediate filaments by cryo-electron tomography. *J.Struct.Biol.* 158:378-385.

Harada, M., S. Sakisaka, K. Terada, R. Kimura, T. Kawaguchi, H. Koga, M. Kim, E. Taniguchi, S. Hanada, T. Suganuma, K. Furuta, T. Sugiyama, and M. Sata. 2001. A mutation of the Wilson disease protein, ATP7B, is degraded in the proteasomes and forms protein aggregates. *Gastroenterology.* 120:967-974.

Harris, K.G., and C.B. Coyne. 2014. Death waits for no man--does it wait for a virus? How enteroviruses induce and control cell death. *Cytokine Growth Factor Rev.* 25:587-596.

Haverkos, H.W., N. Battula, D.P. Drotman, and O.M. Rennert. 2003. Enteroviruses and type 1 diabetes mellitus. *Biomedicine & Pharmacotherapy.* 57:379-385.

He, B. 2006. Viruses, endoplasmic reticulum stress, and interferon responses. *Cell Death Differ.* 13:393-403.

Heath, C.M., M. Windsor, and T. Wileman. 2001. Aggresomes resemble sites specialized for virus assembly. *J.Cell Biol.* 153:449-455.

Heaton, S.M., N.A. Borg, and V.M. Dixit. 2016. Ubiquitin in the activation and attenuation of innate antiviral immunity. *J.Exp.Med.* 213:1-13.

Helfand, B.T., A. Mikami, R.B. Vallee, and R.D. Goldman. 2002. A requirement for cytoplasmic dynein and dynactin in intermediate filament network assembly and organization. *J.Cell Biol.* 157:795-806.

Herrmann, H., and U. Aebi. 2000. Intermediate filaments and their associates: multi-talented structural elements specifying cytoarchitecture and cytodynamics. *Curr.Opin.Cell Biol.* 12:79-90.

Hesse, M., T.M. Magin, and K. Weber. 2001. Genes for intermediate filament proteins and the draft sequence of the human genome: novel keratin genes and a surprisingly high number of pseudogenes related to keratin genes 8 and 18. *J.Cell.Sci.* 114:2569-2575.

Huttunen, M., M. Waris, R. Kajander, T. Hyypia, and V. Marjomaki. 2014. Coxsackievirus A9 infects cells via nonacidic multivesicular bodies. *J.Virol.* 88:5138-5151.

Hyypia, T., T. Hovi, N.J. Knowles, and G. Stanway. 1997. Classification of enteroviruses based on molecular and biological properties. *J.Gen.Virol.* 78 (Pt 1):1-11.

Ivaska, J., H.M. Pallari, J. Nevo, and J.E. Eriksson. 2007. Novel functions of vimentin in cell adhesion, migration, and signaling. *Exp.Cell Res.* 313:2050-2062.

Jheng, J.R., C.Y. Lin, J.T. Horng, and K.S. Lau. 2012. Inhibition of enterovirus 71 entry by transcription factor XBP1. *Biochem.Biophys.Res.Commun.* 420:882-887.

Johnston, J.A., C.L. Ward, and R.R. Kopito. 1998. Aggresomes: a cellular response to misfolded proteins. *J.Cell Biol.* 143:1883-1898.

Johnston, J.A., M.J. Dalton, M.E. Gurney, and R.R. Kopito. 2000. Formation of high molecular weight complexes of mutant Cu,Zn-superoxide dismutase in a mouse model for familial amyotrophic lateral sclerosis. *Proceedings of the National Academy of Sciences.* 97:12571-12576.

Junn, E., S.S. Lee, U.T. Suhr, and M.M. Mouradian. 2002. Parkin accumulation in aggresomes due to proteasome impairment. *J.Biol.Chem.* 277:47870-47877.

Kankaanpaa, P., L. Paavolainen, S. Tiitta, M. Karjalainen, J. Paivarinne, J. Nieminen, V. Marjomaki, J. Heino, and D.J. White. 2012. BioImageXD: an open, general-purpose and high-throughput image-processing platform. *Nat.Methods.* 9:683-689.

Karczewski, M.K., and K. Strebel. 1996. Cytoskeleton association and virion incorporation of the human immunodeficiency virus type 1 Vif protein. *J.Virol.* 70:494-507.

Kawaguchi, Y., J.J. Kovacs, A. McLaurin, J.M. Vance, A. Ito, and T. Yao. 2003. The Deacetylase HDAC6 Regulates Aggresome Formation and Cell Viability in Response to Misfolded Protein Stress. *Cell.* 115:727-738.

Kim, J.K., A.M. Fahad, K. Shanmukhappa, and S. Kapil. 2006. Defining the cellular target(s) of porcine reproductive and respiratory syndrome virus blocking monoclonal antibody 7G10. *J.Virol.* 80:689-696.

Kim, S., and P.A. Coulombe. 2007. Intermediate filament scaffolds fulfill mechanical, organizational, and signaling functions in the cytoplasm. *Genes Dev.* 21:1581-1597.

Knowles, J.N., T. Hovi, A.M. King, and G. Stanway. 2010. Overview of taxonomy. *In* The Picornaviruses. E. Ehrenfeld, E. Domingo and R.P. Roos, editors. ASM Press, Washington DC. 19-32.

Kopito, R.R. 2000. Aggresomes, inclusion bodies and protein aggregation. *Trends Cell Biol.* 10:524-530.

Lansdown, A.B. 1976. Pathological changes in the pancreas of mice following infection with Coxsackie B viruses. *Br.J.Exp.Pathol.* 57:331-338.

Lei, S., Y.P. Tian, W.D. Xiao, S. Li, X.C. Rao, J.L. Zhang, J. Yang, X.M. Hu, and W. Chen. 2013. ROCK is involved in vimentin phosphorylation and rearrangement induced by dengue virus. *Cell Biochem.Biophys.* 67:1333-1342.

Macejak, D.G., and P. Sarnow. 1992. Association of heat shock protein 70 with enterovirus capsid precursor P1 in infected human cells. *J.Virol.* 66:1520-1527.

Marjomaki, V., P. Turkki, and M. Huttunen. 2015. Infectious Entry Pathway of Enterovirus B Species. *Viruses.* 7:6387-6399.

Miller, M.S., and L. Hertel. 2009. Onset of human cytomegalovirus replication in fibroblasts requires the presence of an intact vimentin cytoskeleton. *J.Virol.* 83:7015-7028.

Murti, K.G., and R. Goorha. 1983. Interaction of frog virus-3 with the cytoskeleton. I. Altered organization of microtubules, intermediate filaments, and microfilaments. *J.Cell Biol.* 96:1248-1257.

Nagy, P.D., R.Y. Wang, J. Pogany, A. Hafren, and K. Makinen. 2011. Emerging picture of host chaperone and cyclophilin roles in RNA virus replication. *Virology.* 411:374-382.

Nawrocki, S.T., J.S. Carew, M.S. Pino, R.A. Highshaw, R.H. Andtbacka, K. Dunner Jr, A. Pal, W.G. Bornmann, P.J. Chiao, P. Huang, H. Xiong, J.L. Abbruzzese, and D.J. McConkey. 2006. Aggresome disruption: a novel strategy to enhance bortezomib-induced apoptosis in pancreatic cancer cells. *Cancer Res.* 66:3773-3781.

Nedellec, P., P. Vicart, C. Laurent-Winter, C. Martinat, M.C. Prevost, and M. Brahic. 1998. Interaction of Theiler's virus with intermediate filaments of infected cells. *J.Virol.* 72:9553-9560.

Omary, M.B., P.A. Coulombe, and W.H. McLean. 2004. Intermediate filament proteins and their associated diseases. *N.Engl.J.Med.* 351:2087-2100.

Pastorino, B., E. Boucomont-Chapeaublanc, C.N. Peyrefitte, M. Belghazi, T. Fusai, C. Rogier, H.J. Tolou, and L. Almeras. 2009. Identification of cellular proteome modifications in response to West Nile virus infection. *Mol.Cell.Proteomics.* 8:1623-1637.

Pinkert, S., K. Klingel, V. Lindig, A. Dorner, H. Zeichhardt, O.B. Spiller, and H. Fechner. 2011. Virus-host coevolution in a persistently coxsackievirus B3-infected cardiomyocyte cell line. *J.Virol.* 85:13409-13419.

Prahlad, V., M. Yoon, R.D. Moir, R.D. Vale, and R.D. Goldman. 1998. Rapid movements of vimentin on microtubule tracks: kinesin-dependent assembly of intermediate filament networks. *J.Cell Biol.* 143:159-170.

Ram, B.M., and G. Ramakrishna. 2014. Endoplasmic reticulum vacuolation and unfolded protein response leading to paraptosis like cell death in cyclosporine A treated cancer cervix cells is mediated by cyclophilin B inhibition. *Biochim.Biophys.Acta.* 1843:2497-2512.

Risco, C., J.R. Rodriguez, C. Lopez-Iglesias, J.L. Carrascosa, M. Esteban, and D. Rodriguez. 2002. Endoplasmic reticulum-Golgi intermediate compartment membranes and vimentin filaments participate in vaccinia virus assembly. *J.Virol.* 76:1839-1855.

Rust, R.C., L. Landmann, R. Gosert, B.L. Tang, W. Hong, H.P. Hauri, D. Egger, and K. Bienz. 2001. Cellular COPII proteins are involved in production of the vesicles that form the poliovirus replication complex. *J.Virol.* 75:9808-9818.

Sano, R., and J.C. Reed. 2013. ER stress-induced cell death mechanisms. *Biochimica Et Biophysica Acta (BBA) - Molecular Cell Research.* 1833:3460-3470.

Schnurr, D., and N. Schmidt. 2013. Persistent infections. *In* Coxsackieviruses: A General Update (Infectious Agents and Pathogenesis). M. Bendinelli and H. Friedman, editors. Springer Science & Business Media, New York, US. 181.

Schonthal, A.H. 2012. Endoplasmic reticulum stress: its role in disease and novel prospects for therapy. *Scientifica (Cairo).* 2012:857516.

Schweitzer, S.C., and R.M. Evans. 1998. Vimentin and lipid metabolism. *Subcell.Biochem.* 31:437-462.

Shafren, D.R., D.T. Williams, and R.D. Barry. 1997. A decay-accelerating factor-binding strain of coxsackievirus B3 requires the coxsackievirus-adenovirus receptor protein to mediate lytic infection of rhabdomyosarcoma cells. *J.Virol.* 71:9844-9848.

Shaid, S., C.H. Brandts, H. Serve, and I. Dikic. 2013. Ubiquitination and selective autophagy. *Cell Death Differ.* 20:21-30.

Stefanovic, S., M. Windsor, K.I. Nagata, M. Inagaki, and T. Wileman. 2005. Vimentin rearrangement during African swine fever virus infection involves retrograde transport along microtubules and phosphorylation of vimentin by calcium calmodulin kinase II. *J.Virol.* 79:11766-11775.

Tang, D.D. 2008. Intermediate filaments in smooth muscle. *Am.J.Physiol.Cell.Physiol.* 294:C869-78.

Thomas, E.K., R.J. Connelly, S. Pennathur, L. Dubrovsky, O.K. Haffar, and M.I. Bukrinsky. 1996. Anti-idiotypic antibody to the V3 domain of gp120 binds to vimentin: a possible role of intermediate filaments in the early steps of HIV-1 infection cycle. *Viral Immunol.* 9:73-87.

Toivola, D.M., G.Z. Tao, A. Habtezion, J. Liao, and M.B. Omary. 2005. Cellular integrity plus: organelle-related and protein-targeting functions of intermediate filaments. *Trends Cell Biol.* 15:608-617.

Waelter, S., A. Boeddrich, R. Lurz, E. Scherzinger, G. Lueder, H. Lehrach, and E.E. Wanker. 2001. Accumulation of mutant huntingtin fragments in aggresome-like inclusion bodies as a result of insufficient protein degradation. *Mol.Biol.Cell.* 12:1393-1407.

Ward, C.L., S. Omura, and R.R. Kopito. 1995. Degradation of CFTR by the ubiquitin-proteasome pathway. *Cell.* 83:121-127.

Welch, W.J., and J.R. Feramisco. 1984. Nuclear and nucleolar localization of the 72,000-dalton heat shock protein in heat-shocked mammalian cells. *J.Biol.Chem.* 259:4501-4513.

Wigley, W.C., R.P. Fabunmi, M.G. Lee, C.R. Marino, S. Muallem, G.N. DeMartino, and P.J. Thomas. 1999. Dynamic association of proteasomal machinery with the centrosome. *J.Cell Biol.* 145:481-490.

Wojcik, C., M. Yano, and G.N. DeMartino. 2004. RNA interference of valosin-containing protein (VCP/p97) reveals multiple cellular roles linked to ubiquitin/proteasome-dependent proteolysis. *J.Cell.Sci.* 117:281-292.

World Health Organization, WHO. http://www.who.int/features/qa/07/en/, cited 11.04.2016.

Zhang, H.M., X. Ye, Y. Su, J. Yuan, Z. Liu, D.A. Stein, and D. Yang. 2010. Coxsackievirus B3 infection activates the unfolded protein response and induces apoptosis through downregulation of p58IPK and activation of CHOP and SREBP1. *J.Virol.* 84:8446-8459.

Zhang, K., and R.J. Kaufman. 2004. Signaling the unfolded protein response from the endoplasmic reticulum. *J.Biol.Chem.* 279:25935-25938.

Zhang, L., and A. Wang. 2012. Virus-induced ER stress and the unfolded protein response. *Front.Plant.Sci.* 3:293.